Climate-inferred distribution estimates of mid-to-late Pliocene hominins

Corentin Gibert, Anaïs Vignoles, Camille Contoux, William Banks, Doris Barboni, Jean-Renaud Boisserie, Olivier Chavasseau, Frédéric Fluteau, Franck Guy, Camille Noûs, et al.

Climate-inferred distribution estimates of mid-to-late Pliocene hominins

*Corentin Gibert[1,2*Δ], Anaïs Vignoles[1, Δ], Camille Contoux[3], William E. Banks[1,4], Doris Barboni[5], Jean-Renaud Boisserie[2,6], Olivier Chavasseau[2], Frédéric Fluteau[7], Franck Guy[2], Camille Noûs[8], Olga Otero[2], Pierre Sepulchre[3], Antoine Souron[1], Gilles Ramstein[3]*

[*] *Corresponding author : corentingibert@gmail.com*
[Δ] *Equally contributed, shared first-authorship.*

1. *University of Bordeaux, CNRS, MCC, PACEA, UMR 5199, Bâtiment B2, Allée Geoffroy St. Hilaire, CS 50023, 33600 Pessac, France.*
2. *Paléontologie, Evolution, Paléoécosystèmes, Paléoprimatologie (PALEVOPRIM), CNRS & Université de Poitiers, Poitiers, France.*
3. *Laboratoire des Sciences du Climat et de l'Environnement (LSCE), IPSL, Gif-sur-Yvette, France.*
4. *Biodiversity Institute, University of Kansas, 1345 Jayhawk Blvd, Lawrence, KS 66045, USA*
5. *CEREGE, Aix Marseille Université, CNRS, IRD, INRAE, Aix-en-Provence, France.*
6. *Centre Français des Études Éthiopiennes, Ministère de l'Europe et des affaires étrangères & CNRS, PO BOX 5554, Addis Ababa, Ethiopia.*
7. *Institut de Physique du Globe de Paris (IPGP), Paris, France.*
8. *Laboratoire Cogitamus, Paris, France.*

Abstract

During the mid-to-late Pliocene (ca. 4–3 Ma), several hominin species were present in central Sahel, eastern and southern Africa. Potential discovery of hominin remains from this period is limited by the availability of exposed Pliocene deposits and the ability to investigate them. As a result, most discoveries have been made in the Afar region of Ethiopia and in the Lake Turkana basin, thus unveiling only a portion of Pliocene hominins' probable geographical presence. In this study we provide a continental view of geographic areas potentially accessible to these hominins. To do so, we simulate the climatic envelope suitable for mid-to-late Pliocene hominin presence, using the earth system model IPSL-CM5A and the Maxent habitat suitability algorithm. The latter indicates high habitat suitability for these hominin species in semi-arid regions where annual thermal amplitude and mean annual precipitation are moderate, mostly corresponding to tropical xerophytic shrublands. Our habitat model estimates geographically continuous, suitable climatic conditions for hominins between central Sahel and northeastern Africa, but not between eastern and southern Africa. This discontinuity suggests that southern African and eastern African hominins were separated by an environmental barrier that could only crossed during particularly favourable periods or by undertaking long-range dispersal over climatically hostile habitats. During simulated periods of climate changes driven by orbital precession this climatic barrier is not present. The Turkana basin, the Laetoli region, and a large part of southern Africa remain suitable for all precession angles, suggesting that these areas may have functioned as refugia. The constant presence of these stable areas combined with the periodic establishment of corridors for dispersion can potentially explain hominin diversity in eastern Africa.

Keywords : Habitat suitability model, Niche modeling, *Australopithecus*, Africa, Pliocene, Dispersal

1. Introduction

The mid-to-late Pliocene, ca. 4–3 million years ago (Ma), was a period of global warmth with atmospheric CO_2 concentrations around 400 ppm, smaller ice sheets, reduced desert areas compared to the present, a global temperature 2–3°C warmer than the preindustrial period (e.g. Salzmann et al.; 2013; Haywood et al., 2020). Oxygen isotope ratios of benthic foraminifera and continental ice records show that this period was climatically stable, with the exception of short-lived cold episodes around 3.6 Ma and 3.3 Ma (De Schepper et al., 2014; Lisiecki and Raymo, 2005). During this period, several hominin species appear to have coexisted and fossil occurences occur in three distinct geographic areas: central Sahel (*Australopithecus bahrelghazali*: Brunet et al., 1995, 1996; Lebatard et al., 2008), eastern Africa (*Au. anamensis, Au. afarensis*: Haile-Selassie et al., 2019; *Kenyanthropus platyops*: Leakey et al. 2001; *Au. deyiremeda*: Haile-Selassie et al., 2015) and southern Africa (*Au. prometheus*: Clarke and Kuman, 2019; *Au. africanus*: Dart, 1925; Herries et al., 2013*)*. These hominins thrived in C_3-C_4 mosaic habitats (Behrensmeyer and Reed, 2013), close to freshwater sources in the form of rivers (Curran and Haile-Selassie, 2016), springs and oases (Barboni et al., 2019), or lakes (paleo-lake Turkana: Feibel, 2011; Boës et al., 2019; paleo-lake Chad: Schuster et al., 2009; Lee-Thorp et al., 2012). They may have used technology, since the oldest recovered retouched pebble assemblage discovered near Lake Turkana is dated ca. 3.3–3.2 Ma (Harmand et al., 2015).

While their exploited microhabitats appear to have been mostly dominated by the presence of freshwater and some locally sustained trees, several authors propose that they could have coped with a variety of environments (within which similar microhabitats could occur), thus leading to the idea that the genus *Australopithecus* could have been eurytopic (Bonnefille et al., 2004; Behrensmeyer and Reed, 2013). Our ability, however, to observe and investigate hominin remains from this period is limited by the availability of exposed Pliocene deposits. As a result, most discoveries have been made in the Afar region of Ethiopia and the Lake Turkana Basin, thus representing only a portion of the probable Pliocene hominin geographic distribution. Here, we aim to provide a continental view of the geographic areas potentially accessible to these hominin populations. Reconstructing the presence of freshwater sources at reduced geographic scales is speculative for chronological intervals that have a resolution of hundreds

of thousands of years and regions for which detailed paleotopography is unknown. However, sources of perennial freshwater and associated gallery vegetation can occur anywhere total annual precipitation exceeds 200–300 mm and topographic depressions or river channels exist (Quade et al., 2018). This is the case during the mid-Holocene and the Last Interglacial when surface drainage was reactivated in the Sahara (e.g. Coulthard et al., 2013; Skonieczny et al., 2015), as well as in areas where precipitation is lower than that threshold, but sustained by groundwater (e.g. present-day Ounianga lakes in northeastern Chad: Kröpelin et al., 2008). C_3-C_4 mosaic habitats, similar to those occupied by hominins, are ubiquitous in African savannah environments (Marston et al., 2018) for which woody cover depends on the frequency and intensity of single rainfall events (Good and Caylor, 2011), which are not known for past periods. Although there is a link between large-scale climate and hominid microhabitats, i.e., perennial freshwater sources enable the development of mosaic habitats, we cannot mechanically calculate this.

We address these issues from a statistical point of view by employing climate envelope modeling methods to determine which large-scale climate variables are most appropriate for explaining known hominin occurrences between 4 Ma and 3 Ma and inferring their potential distributions. To do so, we employ a set of mid-to-late Pliocene climatic variables simulated with the earth system model IPSL-CM5A (Dufresne et al., 2013) to create a climatic envelope model that best matches the distribution of mid-to-late Pliocene hominin occurrences using the *kuenm* R package (Cobos et al., 2019), which uses the Maxent algorithm (Phillips et al., 2006, 2017). Via this approach, we 1) evaluate the capacity of these methods to diagnose the appropriate areas for which we possess data; 2) map potentially suitable areas currently free of paleontological remains and 3) employ a series of insolation sensitivity experiments to investigate potential dispersal between our targeted geographic regions and potential refuge areas.

2. Methods

2.1 Climate model description and setup

We use the earth system model IPSL-CM5A to simulate late Pliocene climate. Atmospheric resolution of the model is 3.75° in longitude by 1.9° in latitude, with 39 vertical levels. Mean grid spacing of the ocean model is approximately 2°, while latitudinal resolution is refined to 0.5° near the equator and 1° in the Mediterranean Sea. This model has been widely used for the study of future and past climates (e.g. Dufresne et al., 2013; Kageyama et al., 2013; Contoux et al., 2012, 2015). The boundary conditions used to force the model follow the Pliocene Model Intercomparison Project phase 1 (PlioMIP1) guidelines described by Haywood et al. (2010). They have been adapted to the IPSL-CM5A model with a modified topography, smaller ice sheets, and atmospheric concentration of CO2 fixed at 405 ppm (Contoux et al., 2012). The climate model uses PlioMIP boundary conditions designed to simulate the climate of the mid-Piacenzian (Contoux et al., 2012). Given that benthic isotope ratios show that climate variability was low from 4–2.8 Ma except for two cold outbursts at 3.6 and 3.3 Ma (Lisiecki and Raymo, 2005; Tan et al., 2017), we extrapolate that this simulation is valid for the period between 4–3 Ma, which mostly corresponds to the Piacenzian. There exists a multitude of possible orbital configurations for any period that spans several hundred thousand years, but we can only use one set of orbital parameters per simulation since we conduct equilibrium climate simulations rather than transient ones. Because the primary goal of the PlioMIP simulation was to compare the climate of the mid-Piacenzian to the preindustrial, the choice made by the PlioMIP community was to use the present-day orbital configuration. This present-day configuration is one for which eccentricity is small. In other words, climate variability linked to precession, which is the main mode of climate variability during the Pliocene, is also small. Thus, we use it as a proxy for Pliocene ‘mean’ climate. This simulation (Pliocene ‘mean’ climate) has been extensively studied and compared to other climate models in the framework of PlioMIP1 (e.g. Haywood et al., 2010; Zhang et al., 2013). We also conducted four additional Pliocene experiments in order to capture an envelope of maximum climate variability during our target period. We do so using modified orbital parameters corresponding

to the period of highest eccentricity (see appendix 1) with four different precession angles (one per simulation), corresponding to the Earth at perihelion at the Northern Hemisphere summer solstice (PlioMax June) and autumn equinox (PlioMax September), and the two opposites, at aphelion at Northern Hemisphere summer solstice (PlioMin June) and autumn equinox (PlioMin September). Orbital parameters were calculated using the Analyseries software (Paillard et al., 1996). Climatological means were calculated from the last 50 years of each simulation. Bias correction of the climate model output was obtained by using the climatic anomalies (temperature difference and percent change for precipitation, e.g. Hély et al., 2009) superimposed on Climate Research Unit climate observations at 0.5° by 0.5° (New et al., 2002). This is possible since the biases of a climate model are supposed to be stationary through different time periods (Krinner and Flanner, 2018). Our simulated climatic fields are thus downscaled from a resolution of 1.9° by 3.75° to 0.5° by 0.5°.

2.2 Vegetation model description and setup

We employed the BIOME4 model (Kaplan et al., 2003) to calculate vegetation in equilibrium with the Pliocene mean climate and the four orbital Pliocene climates. To do so, we calculated climate anomalies between each Pliocene experiment and the preindustrial control experiment (temperature difference and percentage of change for precipitation and clouds, e.g. Hély et al., 2009) interpolated at 0.5°x0.5°. The anomalies were then added to the 0.5°x0.5° gridded data from the Climate Research Unit (New et al., 2002). The model BIOME4 calculates vegetation types in equilibrium with climate model outputs (monthly mean precipitation, air surface temperature, cloud cover and absolute annual minimum air surface temperature). Atmospheric CO_2 concentration was fixed at 405 ppm (PlioMIP value) and soil characteristics kept at present-day values.

Biomes are assigned according to which plant functional types (PFT) are dominant, as well as the productivity and leaf area index (LAI) of each PFT. For example, when the productivity on one grid cell is dominated by the the tropical raingreen tree PFT, followed by the C_4 tropical grass and the woody desert PFT, the grid cell will be associated with tropical xerophytic shrubland biome if the LAI of the

tropical raingreen tree PFT is < 4 and to the tropical savannah biome if the LAI of tropical raingreen tree PFT is > 4.

2.3 Hominin occurrence data

Predictive architectures used to estimate ecological niches or climatic envelopes rely, in part, upon the geographic coordinates (longitude and latitude) of locations where the target population has been observed. In this study, the occurrence data are the locations where fossil hominins dated from ca. 4–3 Ma have been recovered. This choice was made for several reasons. First, our climate model is representative of Piacenzian climate (ca. 3.6—2.8 Ma). This corresponds to the chronological interval to which *Au. afarensis* has been dated. Climatic envelope modeling is performed typically at the species level. However, the diversity of Australopithecus species is poorly constrained as some species, and even genera, are controversial *(Au. bahrelghazali, Au. prometheus, K. platyops*). The intra-specific and inter-specific variability of Australopithecus species is also poorly understood, such that with the recent discovery of the first complete cranium of *Au. anamensis* (Haile-Selassie et al., 2019) remains previously assigned to *Au. afarensis* were reclassified as *Au. anamensis*. Given the taxonomic uncertainty of many *Australopithecus* remains, and considering that the genus provides a working framework, we chose to simulate the climatic envelope suitable for the ensemble of Pliocene *Australopithecus* species, as well as *Kenyanthropus*. This approach is justified by the review of *Australopithecus* paleoenvironments carried out by Behrensmeyer and Reed (2013) demonstrating that these hominins are all associated with similar environments, thus suggesting that their climatic envelopes were likely similar. We excluded the more primitive *Ardipithecus*, which is older than 4 Ma, as well as *Australopithecus* species that are clearly Pleistocene in age (*Au. garhi* and *Au. sediba*) since climatic deterioration due to the Northern Hemisphere Glaciation was already well established by that time (e.g. Tan et al., 2018).

In order to have independent training and test data sets and to limit spatial auto-correlation, we eliminated multiple occurrences such that a grid cell (0.5° by 0.5°) only contained a single occurrence point (see below). As a result, we have only 18 occurrence points (Table 1) despite the fact that more

than 18 paleontological sites exist. Most of these localities are tightly clustered, especially in the Awash Valley and the Turkana Basin.

Table 1. Hominin occurrence points used in this study. The sites of Assa Issie (*Au. anamensis*), Aramis (*Ardipithecus* and *Au. anamensis*), Maka and Belohdelie (*Au. afarensis*) and Bouri (*Au. garhi*) all fall in the grid cell 'Middle Awash' because of their geographic proximity.

Occurrence point	Lon (°)	Lat (°)	Age (Ma)	Age reference
Koro-Toro	19.0	16.0	3.5—3	Brunet et al., 1995; Lebatard et al., 2008
Woranso-Mille	40.5	11.5	3.8—3.3	Deino et al., 2010; Haile-Selassie et al., 2012, 2015; Saylor et al., 2019
Hadar & Dikika	40.5	11.0	3.5—2.9	Behrensmeyer and Reed 2013; Alemseged et al., 2006
Middle Awash	40.5	10.5	4.2—3.4	White et al., 1993, 2006a; Renne et al., 1999
Galili	40.5	9.5	4.5—3.5	Kullmer et al., 2008
Usno	36.0	5.5	ca. 3.4	White et al., 2006b
Shungura	36.0	5.0	3.5—3	Brown et al., 2013
Fejej	36.5	4.5	4—3.6	Kappelman et al., 1996; Fleagle et al., 1991
Koobi Fora	35.5	4.0	4.3—2.7	Brown et al., 2013
Allia Bay	36.5	4.0	4.1—3.8	Behrensmeyer and Reed, 2013
Lomekwi	36.5	3.5	3.5	Leakey et al. ,2001
Lothagam	36.0	3.0	ca. 3.5	Leakey and Walker, 2003
Kanapoi	36.0	2.5	4.2—4	Leakey et al., 1998; Ward et al., 2013
Kantis	36.5	-1.5	3.5—3.4	Mbua et al., 2016
Laetoli	35.0	-3.5	3.8—3.4	Su and Harrison, 2008
Makapansgat	29.0	-24.0	3.4—2.6	Herries et al., 2013
Sterkfontein (member 2)	27.5	-26.0	3.6—3	Bruxelles et al., 2019
Taung	24.5	-27.5	3—2.6	Herries et al., 2013

2.4 Maxent climate envelope model and kuenm R package descriptions and set-up

We use the term "climatic envelope modelling" to describe our approach. This term expresses the idea that "a multivariate space of climatic variables best matching the observed species' distribution is being estimated" (Araujo and Peterson, 2012). It does not imply a direct link with Hutchinson's theory of ecological niches, as is the case with the term "ecological niche modeling". In this study, we assume that aspects of climate determine, at least in part, species distributions, and we do not interpret the resulting predictions within a strict ecological niche framework. The output from the Maxent model is termed habitat suitability index. This term of habitat should not be interpreted in the sense of microhabitat because the climatic data that we provide Maxent are at a large scale of 0.5° (i.e. roughly 2500 km^2). The term habitat suitability index should be understood as a measure of how suitable the large-scale environment was to the targeted African Pliocene hominins.

To model the climatic envelope, we use the Maxent algorithm (Phillips et al., 2006, 2017; Phillips and Dudik, 2008), which has shown to perform well compared to other correlative predictive

architectures, especially when relying on limited occurrences datasets (e.g. Phillips et al., 2006; Elith et al., 2006; Hernandez et al., 2006). Maxent requires the geographic location of sites where the target species have been observed (i.e., fossil localities) and geographically continuous environmental variables over the region of interest, which are derived from the climate model described above.

Maxent is based on the maximum entropy principle such that the estimated probability distribution is constrained by climatic characteristic associated with the known occurrence localities while it avoids assumptions not supported by the data. Maxent is not a classical presence-absence modeling method, but rather a presence-background method as real absences are not known and cannot be taken into account during the sampling of environmental variables (Guisan et al., 2017). This approach to background sampling makes Maxent suitable for making distributional predictions based on paleontological data. Maxent will compare the probability distribution associated with presence occurrences with the one associated with background points randomly sampled in the environment. The area over which this comparison will be done (i.e. the calibration area) has a great influence on model performance. Its size should be neither too small or too large (e.g. VanDerWal et al., 2009), and should be biologically meaningful to ensure that the background points represent the environmental conditions accessible to the species (Anderson and Raza, 2010; Barve et al., 2011). The calibration area encompassing all occurrences points and used in Maxent models can be found in Appendix 1. Maxent, however, is known to be sensitive to model settings (e.g. parameterization, number of variables) that affect model complexity (Warren and Seifert, 2011; Peterson et al., 2018). The more complex a model is, the more likely it will be overfitted. The more overfitted a model is, the more it will struggle to extrapolate suitable habitats outside areas where occurrences are already known (Peterson et al., 2007).

In order to address this sensitivity and select the optimal parameterization, we employed the *kuenm* R package (Cobos et al., 2019) to produce and evaluate candidate models, as well as to perform final evaluations of the best models. We performed model calibration by testing the performance of 2210 candidate models. We produced these models using 26 distinct variable sets, made up of all unique combinations of two or more of the five climatic and vegetation variables from the Pliocene ‘mean’ climate simulation descibed below. The candidate models also employed one of 17 regularization multipliers (0.1–1 at intervals of 0.1, 2–6 at intervals of 1, as well as 8 and 10), and five feature classes

241 or feature class combinations (q, qp, lp, lq, lqp; l=linear, q=quadratic, p=product). We based our
242 evaluations of the candidate models' performance by first evaluating significance and predictive power
243 using partial ROC (500 iterations, and 50% of data for bootstrapping; Peterson et al., 2008) and omission
244 rate metrics. We then evaluated model complexity using the Akaike Information Criterion for small
245 sample sizes (AICc) (Warren and Seifert, 2011). We retained model parameterizations that resulted in
246 statistically significant models, resulted in omission rates lower than 5%, and ΔAICc values less than
247 two. The parameters of these retained models were used to create final models with 10 replicates by
248 bootstrapping. The complete *kuenm* R script that used the Pliocene 'mean' climate model is provided as
249 an Rmarkdown document in Appendix 2. The final model was projected onto the sets of environmental
250 conditions for each of the four precession angle configurations. During the process of model projection,
251 we allowed free extrapolation given the response curves (i.e., response curves not truncated for at least
252 two variables) observed during model calibration. In order to consider, the risks associated with strict
253 extrapolation and to prevent misinterpretation of transferred areas with non-analogous conditions, we
254 employed the mobility-oriented parity (MOP) metric (Owens et al., 2013). Following the approach
255 suggested by Pearson et al. (2006) for small sample sizes, the simulated climatic envelope represents
256 "regions that have similar environmental conditions to where the species is known to occur, and not as
257 predicting actual limits to the range of a species", given that absence of proof is not the proof of absence
258 (see Discussion). The lower threshold for hominin presence was set to the value of the lowesthabitat
259 suitability index (fixed sensitivity; Peterson et al., 2011: p.119) score amongst the occurrence points.
260 The five variables used for predicting the envelope model are representative of mean climate
261 and seasonality: Warmest Month Temperature (WMT), Coldest Month Temperature (CMT),
262 Temperature Difference between the warmest and the coldest months (DT), Mean Annual Precipitation
263 (MAP), and Driest Month Precipitation (DMP). Mean Annual Temperature (MAT), Wettest Month
264 Precipitation (WMP), Precipitation Difference between the wettest and the driest months (DP) and Net
265 Primary Productivity (NPP) were excluded from the final analysis, following the recommendations of,
266 e.g. Merow et al., (2013), because they contributed only marginally to the definition of the climatic
267 envelope and were highly correlated to the employed variables. The candidate models used to build the

final model do not necessarily include all of the five selected variables as model overfitting increases with the number of employed environmental variables (Guisan et al., 2017).

Given the chronological uncertainty associated with hominin fossil contexts and the temporal span of the targeted period, we cannot associate specific fossils or groups of fossils with a particular orbital configuration. The most conservative choice is to use the least extreme orbital configuration—Pliocene 'mean' climate—to estimate a climatic envelope. With this configuration, eccentricity is small thereby favoring lower seasonality and lower climatic variability linked to precession. To detect suitable areas that remained stable across the four precession configurations (i.e. refugia), we thresholded the final model and each projection by reclassifying as non-suitable (i.e. 0) all grid cells with suitability scores lower than the lowest value amongst the occurrence points. Next, suitability scores were grouped into three equal categories (low-, mid- and high-suitability areas) to facilitate the reading of the models' geographic projections and prevent direct interpretations of suitability values. Finally, a binary model was computed by reclassifying all suitable grid cells as one and non-suitable cells as zero. We then compared the four obtained binary predictions with the main Pliocene 'mean' climate model to reveal temporally stable areas of suitability.

2.5 Temporal and spatial sampling sensitivity tests

In order to test the sensitivity of our climatic envelope model to the chosen temporal window with respect to occurence sampling, we replicated the approach described above by removing the oldest and most recent Australipthecus taxa from the dataset (i.e. *A. anamensis*, *A. africanus*, *A. prometheus*). The localities, Lomekwi, Kanapoi, Makapansgat, Sterkfontein and Taung, are removed from model computation, resulting in the loss of all South African occurrences. The map of habitat suitability corresponding to this sensitivity test is available in Appendix 1. As recommended for small occurrence datasets (Pearson et al., 2006; Shcheglovitova and Anderson, 2013), we used a delete-one jackknife approach (or leave one out approach) to evaluate the influence of individual occurence on predictive variability. We removed one locality from the dataset, computed the model with $n - 1$ localities in *kuenm* and repeated this process until every locality have been removed once (i.e. n separate models

for *n* observed localities). The *n* projections of these *n* models, as well as a consensus of all projections, are available in Appendix 1.

3. Results

3.1 Climate model validation

First, we assess the validity of the climate model at hominin sites by comparing paleoenvironmental reconstructions to the biome simulated with the BIOME4 model using IPSL-CM5A climate variables (see Supplementary Material). Vegetation reconstructions at hominin sites describe a seasonal, dry mosaic of woodland, shrubland and grassland (Behrensmeyer and Reed, 2013 and references therein), with small-scale more mesic environments sustained by local water resources (e.g. microhabitats sustained by rivers, lakes and springs; see Barboni et al., 2019). The BIOME4 model indicates tropical xerophytic shrubland, tropical savannah, or tropical deciduous woodland at 16 of the 18 hominin localities (Fig. 1, see also Methods). In the BIOME4 model, productivity is higher in tropical deciduous woodland (Kantis locality) than in tropical savannah (Usno and Laetoli localities), and in tropical savannah than in tropical xerophytic shrubland (e.g. Awash Valley, Koro-Toro locality), but the same plant functional types are present in these three biomes. These biomes describe a mix of tropical raingreen trees, C_4 tropical grass, and woody desert plant functional types (C_3 and C_4) that correspond to a warm, seasonally dry climate, which is in good agreement with the

316 mosaic of woodland, bushland and grassland inferred from vegetation reconstructions, although local-
317 scale water sources are invisible to the model.

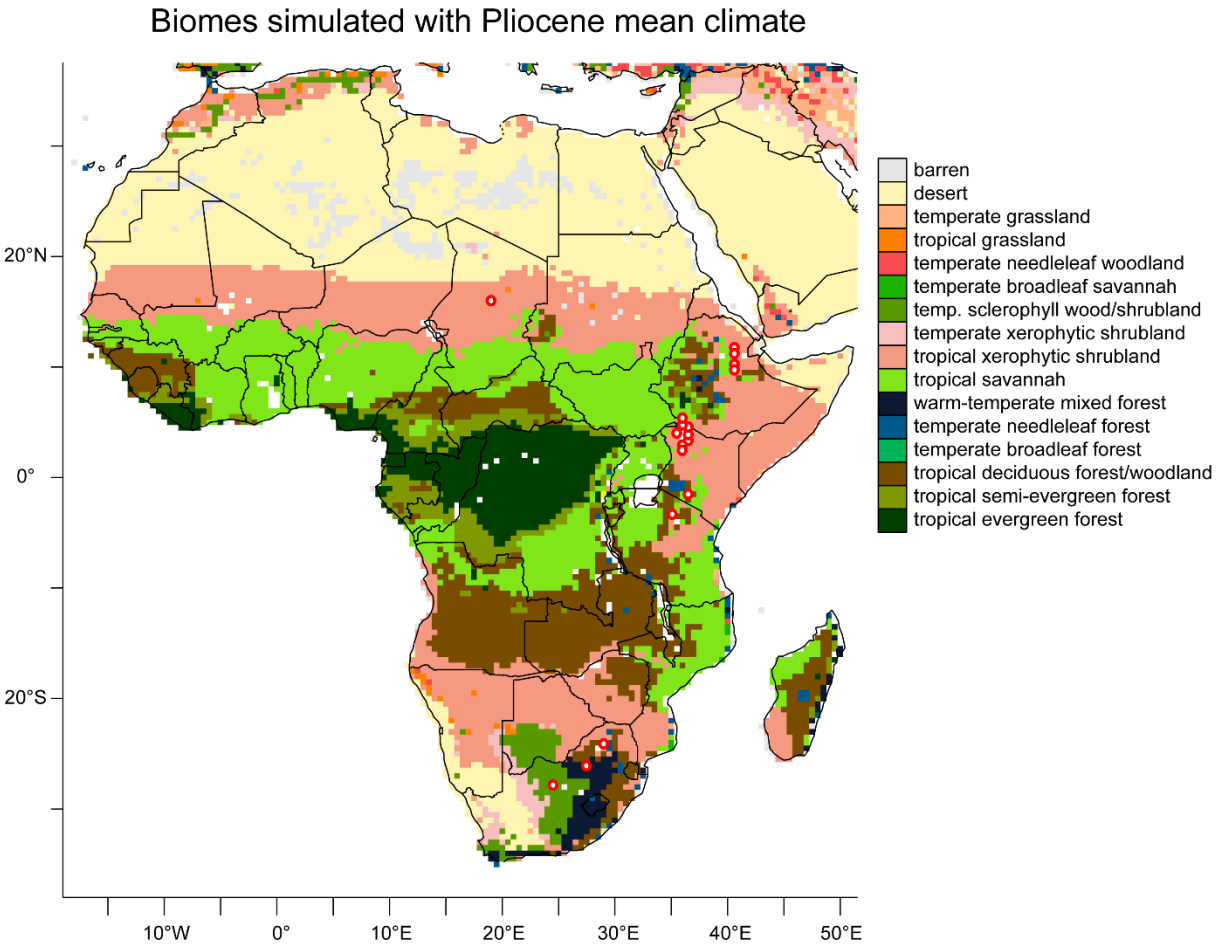

318
319
320 Figure 1. Vegetation simulated with BIOME4 for the Pliocene mean climate. Red circles are the 18
321 hominin occurrence points.
322

323 ### *3.2 Hominin climatic envelope estimations and robustness*

324 At a regional scale, the highest habitat suitability areas reconstructed by the climatic envelope
325 model are located in tropical eastern Africa, except over eastern Somalia and western Ethiopia (Fig.
326 2). The Turkana Basin, areas west of Lake Victoria, as well as a region covering southern Somalia,
327 eastern Kenya and northern Tanzania (including Laetoli and coastal regions, hereafter called the SKT
328 region), and finally western Eritrea, northern Somalia-Djibouti and eastern Ethiopia (including the
329 Awash valley) are the most climatically suitable regions for *Australopithecus*. Three other regions
330 show reasonable habitat suitability indices. The first is a latitudinal corridor at ca. 15°N, covering
331 Africa from the Atlantic coast to the Red Sea, at roughly the latitude of Lake Chad. This Sahelian

corridor suggests a probable continuity of environmental conditions between the Awash valley and the Lake Chad region, with the potential for population dispersals within this corridor. The second area of interest is located in South Africa, southwestern Angola, Botswana, non-coastal Namibia, southern Mozambique, and southeastern Zimbabwe. This area is not connected to eastern Africa in our model, suggesting that population dispersals to or from this southern African area would not have been possible under mean Pliocene climate conditions. The last area is located on the African Mediterranean coast, including the locality of Ain Boucherit, where no Pliocene hominins have been recovered to date, but where stone artefacts and cut-marked bones dating to ca. 2.4 Ma are documented (Sahnouni et al., 2018). Our geographic coverage also includes southern regions of Eurasia (e.g. Yemen, Israel, Jordan, parts of southern Europe) for which habitat suitability attains values suggesting that mid-to-late Pliocene hominins could have survived in these regions if they had been accessible. After *kuenm* calibration process, the final model meeting significance and complexity requirements (of 2210 candidate models) is based on two of the five available variables: the temperature difference between the warmest and the coldest month (DT) and mean annual precipitation (MAP). All hominin occurrences are located in regions where annual precipitation is below 800 mm/yr with a marked dry season and limited annual thermal amplitude (up to 15°C; Fig. 3) inside semi-arid zones (BS in the Köppen-Geiger classification, Peel et al., 2007).

Sensitivity tests on the occurrence data (i.e., leave one out approach) reveal that habitat suitability in the Sahelian corridor is not governed by a single locality, not even Koro-Toro located in central Sahel, while the suitable area in northern Africa is a result of climatic similarities to occurrence points located in eastern Africa (e.g. the Middle Awash) or in southern Africa (e.g. Taung; see Suppl. Fig. 1). The Allia Bay locality in Kenya has the strongest influence on suitability scores in the Sahelian corridor, but even its removal is insufficient to make this pattern disappear. The consensus map (see Suppl. Fig. 1), which combines all the sensitivity tests, demonstrates the robustness of the depicted pattern for hominins in Pliocene 'mean' climate (Fig. 2) by preserving the three main areas of suitable habitats (i.e. eastern, southern Africa, and the Sahelian corridor).

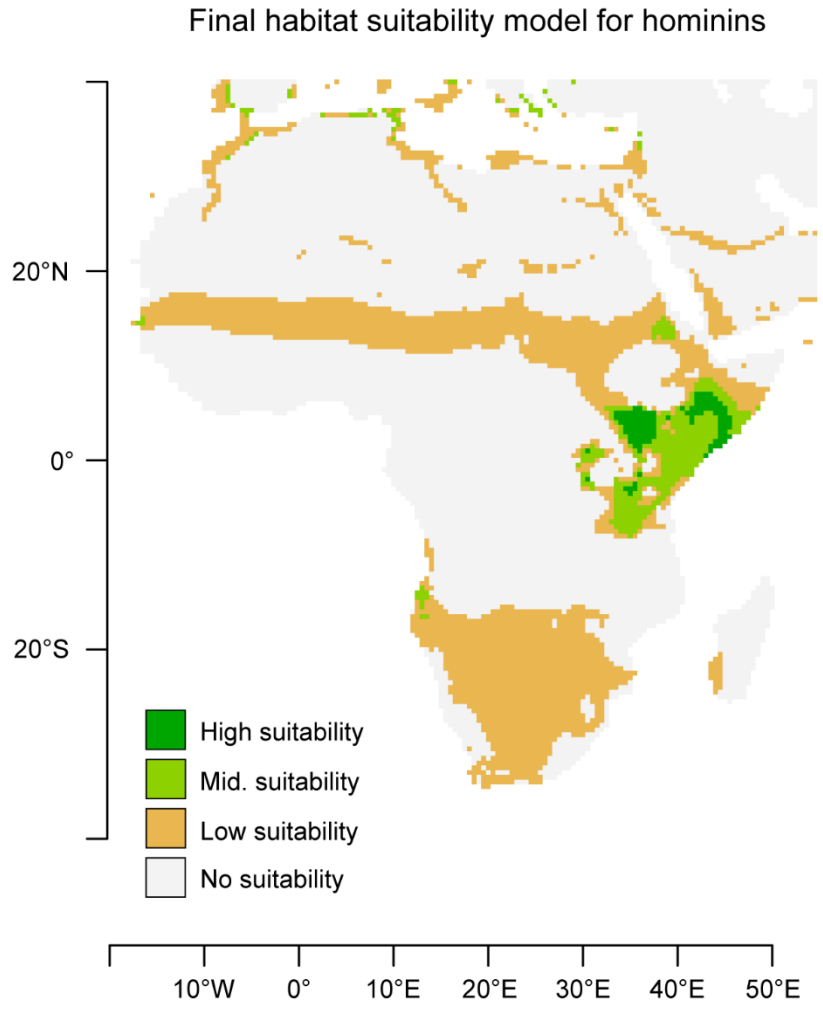

Figure 2. Habitat suitability index for hominins under the Pliocene mean climate scenario. All values above the lowest presence threshold are shown (see Methods). Low suitability regroups cells with habitat suitability values ranging from 0.08–0.36; middle suitability range from 0.36–0.63; and high suitability is assigned to cells with values over 0.63. The final *kuenm* model is based on the DT and MAP variables.

The sensitivity test conducted via temporal sampling (i.e. the removal of youngest and oldest species; see Suppl. Fig. 2) demonstrates the robustness of the climate envelope modeled with all selected occurrences (Fig. 2). We performed this test without the three localities from South Africa and nevertheless the same areas remain suitable for hominins. The main differences between this sensitivity test and the main model are the absolute suitability values in suitable areas. In southern Africa, the eastern coast depicts middle and high suitability in the sensitivity test while in the main model these areas are associated with low suitability scores. In northern Africa and the European Mediterranean coast, suitability values are higher in the test, while conversely the areas of middle and high suitability in eastern Africa are more geographically limited than in the main model.

Our results show that eastern and southern Africa were not connected, with respect to suitability, under Pliocene mean conditions. However, we know that *Australopithecus* was present both in eastern and southern Africa, indicating that either: 1) climate variability allowed them to cross this environmental barrier; or 2) they were able to reach/occupy both regions because their niche was in fact broader or because they attempted long-range dispersal across climatically unsuitable areas. In an effort to evaluate the first hypothesis, we further examined potential geographic variability of suitable areas for mid-to-late Pliocene hominins caused by orbital precession changes.

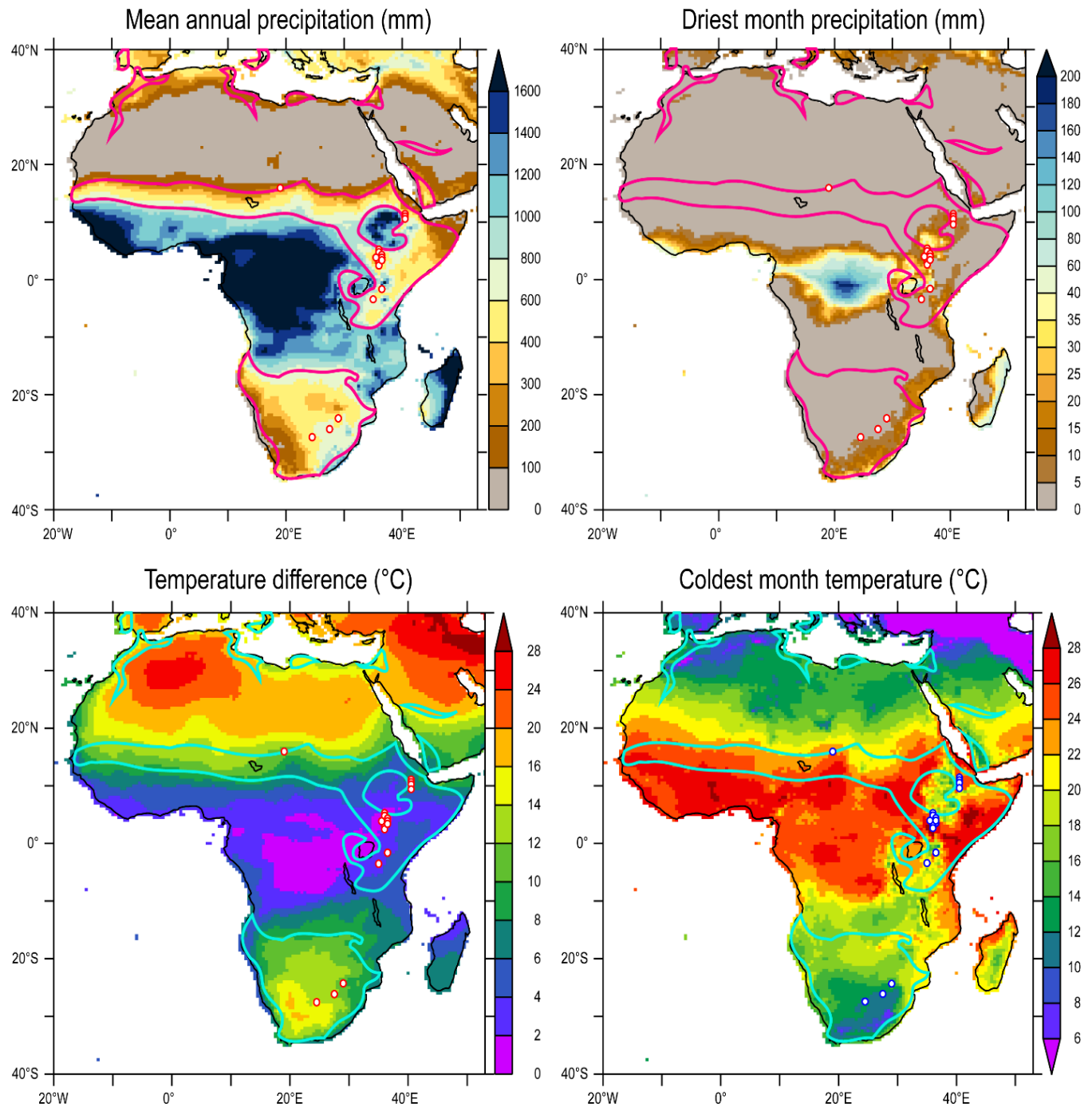

Figure 3. Mean annual precipitation (MAP), driest month precipitation (DMP), temperature difference between the coldest and warmest months (DT), and coldest month temperature for the Pliocene (CMT). Areas suitable for hominins from figure 2 are outlined. MAP and DT are the variables composing the "best" parameter setting selected after model calibration.

391 *3.3 Orbitally driven climate variability and potential dispersals*

392 We projected the climatic envelope estimated from Pliocene mean climate conditions onto four
393 Pliocene climate scenarios simulated with summer and autumn insolation maxima and minima (Figure
394 4, Suppl. Fig. 3-6). This provides examples of the potential ability of Pliocene hominins to disperse

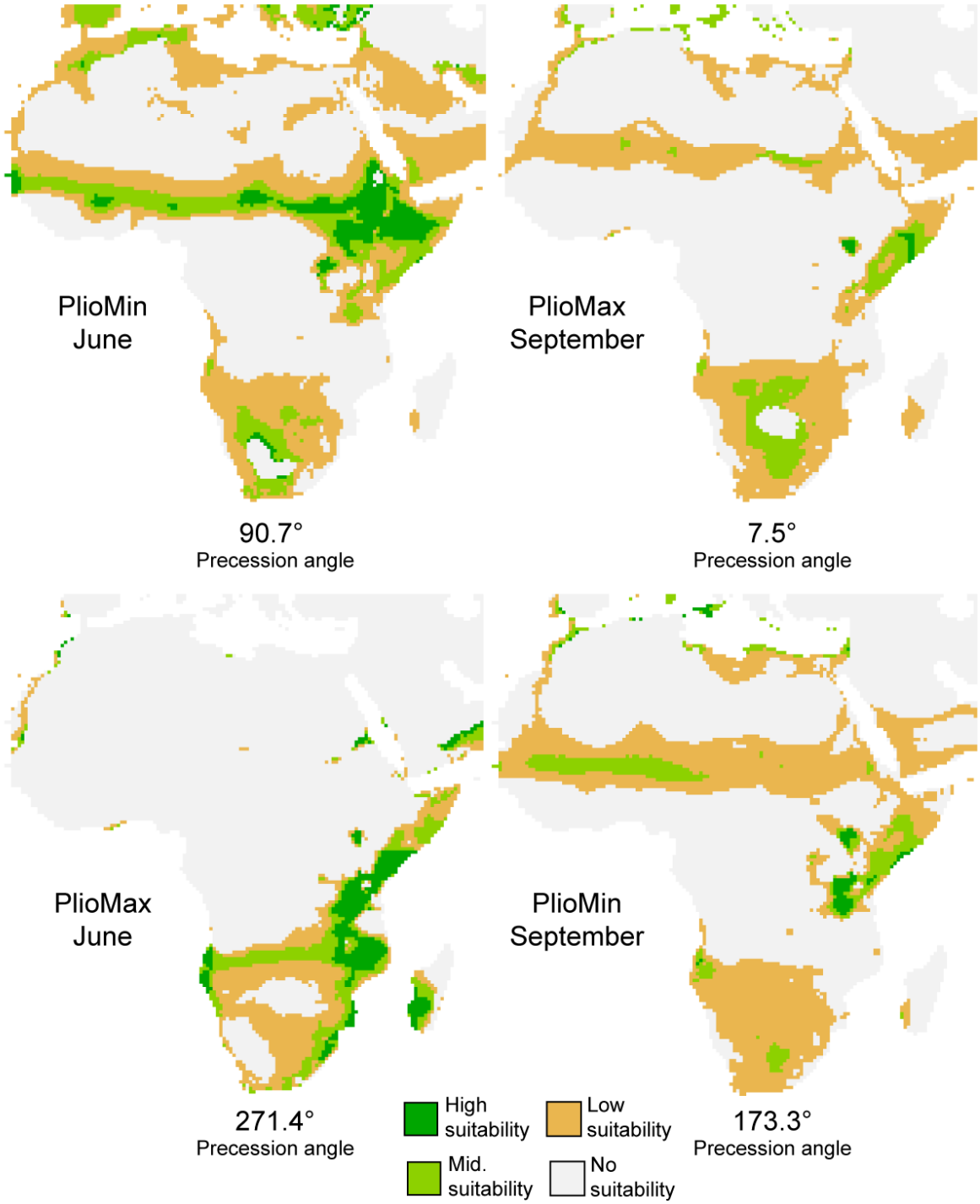

395 Figure 4: Projections of the final model computed with the Pliocene mean configuration onto four
396 orbital precession configurations (see Methods). PlioMax June with a precesion angle of 271° is the
397 most distant configuration from Pliocene 'mean' climate (i.e. 100.04°), whereas PlioMin June is the
398 closest (90.74°).

399 geographically during specific climate scenarios driven by orbital precession variability—dispersals
400 that would not necessitate them changing the environmental conditions they exploited.

401 During periods of boreal summer or autumn insolation maxima (PlioMax June simulation and
402 PlioMax September simulation, respectively), the Afar region and a large portion of eastern Africa are
403 unsuitable, except for the Turkana region and the SKT region (including the Laetoli and coastal
404 regions) (Fig. 4). During these periods, the tropical rain belt is located further north. The Sahelian
405 band of suitability is shifted north of Koro-Toro (Suppl. Fig. 5) into the present-day Sahara for
406 PlioMax September, and it is totally absent for PlioMax June. There remains a large unsuitable area
407 between Laetoli (the southernmost eastern African site) and Makapansgat (the northernmost southern
408 African site) for three of the configurations. However, in the PlioMax June projection (i.e. boreal
409 summer maxima), a continuous zone of middle and high climatic suitability between eastern and
410 southern Africa emerges (Fig. 4, bottom left), which would have allowed hominin dispersal to/from
411 the south. Variations in precession angle could therefore be a potential factor controlling the
412 emergence of corridors permitting the dispersion of ancient hominins between eastern and southern
413 Africa along the Kingdon line (Kingdon, 2003; Joordens et al., 2019). During periods of boreal
414 summer insolation minima (Fig. 4, top left, PlioMin June), the habitat suitability indices becomes high
415 in the northern part of the African rift, particularly in the Ethiopian highlands, down to the Baringo
416 locality and also extend down to Laetoli through the SKT region. Suitability in the Sahelian band
417 increases strongly and shifts southward following the tropical rain belt. Three areas remain above the
418 lowest presence threshold for all orbital configurations and can therefore be considered true core areas
419 or refugia (Fig. 5)—the Turkana Basin, the SKT region, and a vast portion of southern Africa. To the
420 contrary, the Sahelian band and the Awash Valley remain suitable in some, but not all, of the four
421 climate scenarios.

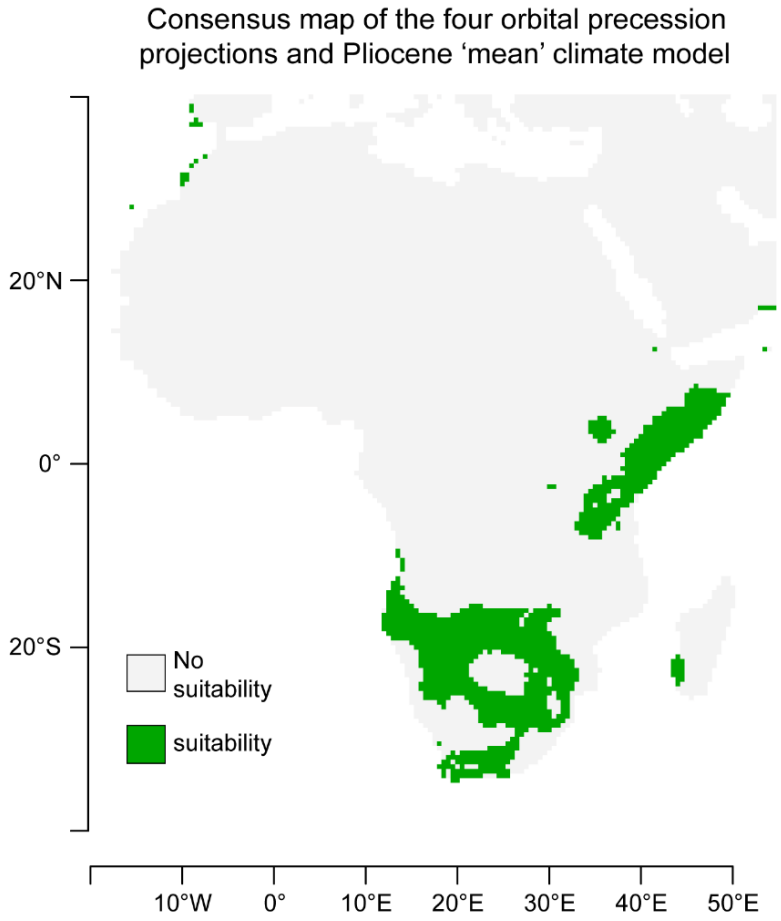

422

423 Figure 5: Refuge areas. Consensus map based on the final climatic envelope's suitable areas estimated
424 with Pliocene 'mean' climate (Fig. 2), as well as with the four orbital precession configurations (Fig.
425 4).

426

427 ## ***4. Discussion***

428

429 ### *4.1* Australopithecus *in semi-arid climate*

430 From the late Miocene onwards, early hominins were not found in sites sampling densely forested
431 environments nor shadowless plains, but instead are known from more or less wooded, mosaic habitats
432 (see Sponheimer 2013). The earliest known hominin, *Sahelanthropus tchadensis*, lived in a Sahelian-
433 like mosaic landscape close to lake settings (Vignaud et al., 2002; Le Fur et al., 2009; Blondel et al.,
434 2010; Novello et al., 2017). The early Pliocene hominins *Ardipithecus ramidus* and *Ardipithecus*
435 *kadabba* are also thought to have lived in an open, wooded savannah biome (Levin et al., 2008; White
436 et al., 1994, 2009; Cerling et al., 2011), within which they occupied localized forested micro-habitats

sustained by springs (WoldeGabriel et al., 2009; Barboni et al., 2019). However not all early hominids are associated with savannahs, *Orrorrin* lived in an open deciduous forest, punctuated by very wet areas (Bamford et al., 2013; Senut, 2020).

By the late Pliocene, *Australopithecus* occupied open landscape environments. Pliocene hominin localities of the Lower Awash Valley and the Turkana Basin had mammal communities corresponding to a climate for which precipitation was low (inferior to 800–1000 mm/yr) and temperature seasonality was pronounced (Robinson et al., 2017). Our model suggests that these populations occupied regions characterized by a semi-arid climate (dry and seasonal with moderate thermal amplitude) and environments that would have been more or less wooded depending on surface and sub-surface water availability. Blumenthal et al. (2017) postulate that variable climatic conditions in the Turkana Basin, within the range of present-day environments, were already present at 4.2 Ma, suggesting that the region's hominins were already occupying (semi-)arid areas with soil temperatures of approximately 30–35°C (Passey et al., 2010). Sponheimer (2013) also states that the australopithecine masticatory apparatus was adapted to abrasive food already by 4 Ma, implying that they could rely on (although perhaps only seasonally) xerophytic tubers which are found in arid environments and can contain up to 70% water. A re-examination of Turkana *Au. anamensis* has shown that C_4 biomass composed up to 30% of their diet, suggesting increased foraging in open landscapes already by 4 Ma (Quinn, 2019). An increased proportion of C_4 foods in the hominin diet occurs at 3.8 Ma (Uno et al., 2016), and *Au. bahrelghazali* was also dependent of C_4-derived resources (Lee-Thorp et al., 2012). At Hadar, *Au. afarensis* was a mixed C_3/C_4 feeder and coped with ecological changes via "… a highly varied intake of C_4 foods" (Wynn et al., 2016). Recent dental analyses of *Au. africanus* also reveal that this species faced seasonal dietary stress (Joannes-Boyau et al., 2019). Finally, our results show that the climate envelope of mid-to-late Pliocene hominins largely overlaps with semi-arid climates, but also includes more temperate climates. This agrees with Behrensmeyer and Reed (2013) who consider that *Australopithecus* could survive "considerable seasonal temperature" variations, thus suggesting that they possessed enhanced thermoregulatory capacities (Lieberman, 2015). This is a step towards the genus *Homo*, which appears to have been adapted to even more arid climates (DiMaggio et al., 2015; Robinson et al., 2017).

4.2 Hypotheses on the paleobiogeography of Australopithecus

Dispersal events during the Pliocene are thought to have strongly influenced the paleobiogeography of *Australopithecus* (Foley et al., 2013). Our results support this hypothesis by indicating that australopithecines in Chad, eastern Africa and South Africa faced similar climatic conditions. However, dispersal between eastern Africa and southern Africa appears to have been possible only during periods of extreme summer insolation (PlioMax June), when the Lake Malawi basin would have been dry enough to create continuous semi-arid environments (Fig. 4 and Suppl. Figure 5). To the contrary, *Au. bahrelghazali*, *Au. afarensis*, and *K. platyops* could have dispersed between the Turkana Basin, Laetoli and the SKT region, the Awash Valley and central Sahel—with the Turkana basin and the SKT region remaining suitable during periods of extreme insolation forcing. Isolation of some regions (e.g., the Turkana Basin and SKT regions serving as refugia), induced by climate and vegetation changes driven by orbital forcing, would have isolated animal populations (including hominids) and reduced gene flow, thus fostering allopatric speciation by vicariance. This would explain the highest levels of species diversity in eastern Africa in that distinct species could develop during periods when the two regions were not connected, and later disperse during periods when they were environmentally linked. Comparing the habitat suitability map to the vegetation model (Figs. 1 and 2), it is evident that areas of suitability correspond primarily to those where the simulated biome is tropical xerophytic shrubland (represented in pink in Fig. 1), although the two maps are not strictly superimposable. This environment is typically present along woodland margins (fringe environments), corresponding to the hypothesis that *Australopithecus* was an edge (or ecotonal) adapted genus (Sussman and Hart, 2015), as suggested for early Pleistocene *Paranthropus robustus* (Caley et al., 2018).

According to our results, the coastal regions of southern Somalia and eastern Kenya would have been suitable even during extreme insolation changes (Fig. 5). This region is included in the extent of the coastal mosaic forest proposed by Kingdon (2003) and Joordens et al., (2019) (the coastal ape hypothesis). However, our vegetation model does not reproduce forest in this area, but rather tropical xerophytic shrubland (this biome does contain the tropical raingreen tree plant functional type); our model also supports the hypothesis that *Australopithecus* did not live in forest contexts, but rather in

493 semi-arid zones. Small-scale patches of gallery forest could have been favoured by local conditions in
494 this area, without being visible in the model, since the coastal forest at present only measures a few
495 tens of kilometres of width at its maximum extent. The fact that occurrence points of Pliocene
496 *Australopithecus* are located in semi-arid areas, which were already semi-arid areas during the
497 Pliocene, does not mean that these species were restricted solely to these areas, since it remains
498 possible that fossils have not been observed elsewhere. Our model, which effectively indicates areas
499 where remains have been recovered, does predict that this region of southern Kenya and northern
500 Tanzania had some tropical trees, and was climatically favourable for *Australopithecus* during the
501 Pliocene even across climate changes linked to orbital precession variability.

502

503 ## ***5. Conclusions***

504

505 During the mid-to-late Pliocene, different hominin species are identified in Africa at localities that
506 are geographically separated (central Sahel, eastern Africa and southern Africa). When using a
507 climatic envelope model, the estimated areas suitable for mid-to-late Pliocene hominins cover most of
508 eastern Africa, the Sahelian corridor from the Atlantic coast to the Red Sea, large portions of southern
509 Africa, and a restricted portion of the African northwestern Mediterranean coast. The climatic
510 envelope associated with these areas is predominantly characterized by strongly seasonal precipitation
511 and annual thermal amplitude up to 15°C, in accordance with the two variables selected by the kuenm
512 R package to create the final model (i.e., mean annual precipitation and thermal amplitude between
513 coldest and warmest month). The estimated envelope is geographically continuous between eastern
514 Africa and the Lake Chad region, while a similar pattern is not observed between eastern Africa and
515 southern Africa, suggesting that this environmental barrier was crossed during periods of extreme
516 summer insolation maxima or that hominins had a broader climatic envelope than the one estimated
517 with our occurrence data. The Turkana Basin, the region covering southern Somalia, eastern Kenya
518 and northern Tanzania (including Laetoli and coastal regions), and a vast portion of southern Africa
519 remain suitable during periods of orbital variability, contrary to the Sahelian corridor and the Awash
520 valley. Those refugia are located in eastern and southern Africa and are only connected during certain

orbital configurations, potentially explaining the diversity of hominin species observed in eastern Africa at that time.

Further studies could improve our results, notably, due to the scarce nature of presently available data, but this is certainly a long-term perspective. For the immediate future, the increased capability of climate models to simulate Pliocene conditions via PLIOMIP2 (Haywood, 2020; Tan et al., 2020; Zhang et al., 2020) warrants pursuing.

6. Acknowledgments

This research was conducted within the framework of the ANR projet HADoC (ANR-17-CE31-0010). The authors were granted access to the HPC resources of TGCC under the allocation 2019-A0050102212 made possible by GENCI.

7. References

Alemseged, Z., Spoor, F., Kimbel, W.H., Bobe, R., Geraads, D., Reed, D., Wynn, J.G., 2006. A juvenile early hominin skeleton from Dikika, Ethiopia. Nature 443(7109), 296–301. https://doi.org/10.1038/nature05047

Anderson, R.P., Raza, A., 2010. The effect of the extent of the study region on GIS models of species geographic distributions and estimates of niche evolution: preliminary tests with montane rodents (genus *Nephelomys*) in Venezuela. J. Biogeogr. 37(7), 1378–1393. https://doi.org/10.1111/j.1365-2699.2010.02290.x

Araújo, M.B., Peterson, A.T., 2012. Uses and misuses of bioclimatic envelope modeling. Ecology 93, 1527–1539. https://doi.org/10.1890/11-1930.1

Ashley, G.M., Barboni, D., Dominguez-Rodrigo, M., Bunn, H.T., Mabulla, A.Z.P., Diez-Martin, F., Barba, R., Baquedano, E., 2010. Paleoenvironmental and paleoecological reconstruction of a freshwater oasis in savannah grassland at FLK North, Olduvai Gorge, Tanzania. Quat. Res. 74(3), 333–343. https://doi.org/10.1016/j.yqres.2010.08.006

Bamford, M., 1999. Pliocene fossil woods from an early hominid cave deposit, Sterkfontein, South Africa. S. Afr. J. Sci. 95, 231–237. https://doi.org/10.10520/AJA00382353_7397

Bamford, M.K., Senut, B., Pickford, M., 2013. Fossil leaves from Lukeino, a 6-million-year-old Formation in the Baringo Basin, Kenya. Geobios 46(4), 253–272. https://doi.org/10.1016/j.geobios.2013.02.001

Banks, W.E., d'Errico, F., Peterson, A.T., Vanhaeren, M., Kageyama, M., Sepulchre, P., Lunt, D., 2008. Human ecological niches and ranges during the LGM in Europe derived from an application of eco-cultural niche modeling. J. Archaeol. Sci. 35(2), 481–491. https://doi.org/10.1016/j.jas.2007.05.011

569 Barboni, D., Ashley, G.M., Bourel, B., Arráiz, H., Mazur, J.-C., 2019. Springs, palm groves, and the
570 record of early hominins in Africa. Rev. Palaeobot. Palynol. 266, 23–41.
571 https://doi.org/10.1016/j.revpalbo.2019.03.004
572
573 Behrensmeyer, A.K., Reed, K.E., 2013. Reconstructing the habitats of *Australopithecus*:
574 paleoenvironments, site taphonomy, and faunas, in: Reed, K.E., Fleagle, J.G., Leakey, R.E. (Eds.),
575 The paleobiology of *Australopithecus*. Springer, Dordrecht, pp. 41–60. https://doi.org/10.1007/978-
576 94-007-5919-0_4
577
578 Blondel, C., Merceron, G., Andossa, L., Taisso, M.H., Vignaud, P., Brunet, M., 2010. Dental
579 mesowear analysis of the late Miocene Bovidae from Toros-Menalla (Chad) and early hominid
580 habitats in Central Africa. Palaeogeogr. Palaeoclimatol. Palaeoecol. 292, 184–191.
581 https://doi.org/10.1016/j.palaeo.2010.03.042
582
583 Blumenthal, S.A., Levin, N.E., Brown, F.H., Brugal, J.P., Chritz, K.L., Harris, J.M., Jehle, G.E.,
584 Cerling, T.E., 2017. Aridity and hominin environments. Proc. Natl. Acad. Sci. USA 114(28), 7331–
585 7336. https://doi.org/10.1073/pnas.1700597114
586
587 Bobe, R., 2011. Fossil mammals and paleoenvironments in the Omo-Turkana Basin. Evol. Anthropol.
588 20, 254–263. https://doi.org/10.1002/evan.20330
589
590 Boës, X., Prat, S., Arrighi, V., Feibel, C., Haileab, B., Lewis, J., Harmand, S., 2019. Lake-level
591 changes and hominin occupations in the arid Turkana basin during volcanic closure of the Omo River
592 outflows to the Indian Ocean. Quat. Res. 91(2), 892–909. https://doi.org/10.1017/qua.2018.118
593
594 Bonnefille, R., Potts, R., Chalie, F., Jolly, D., Peyron, O., 2004. High-resolution vegetation and
595 climate change associated with Pliocene *Australopithecus afarensis*. Proc. Natl. Acad. Sci. USA 101,
596 12125–12129. https://doi.org/10.1073/pnas.0401709101
597
598 Boyd, M.D., Manthi, F.K., Ward, C.V., Plavcan, J.M., 2018. A synthesis of multi-proxy
599 paleoenvironmental reconstruction methods: the depositional environments of the Lomekwi member,
600 Nachukui Formation, West Turkana. AGU Fall Meeting Abstracts 2018, PP31B-1657.
601 http://doi:10.1130/abs/2018AM-319628
602
603 Brown, F.H., McDougall, I., Gathogo, P.N., 2013. Age Ranges of *Australopithecus* species, Kenya,
604 Ethiopia, and Tanzania, in: Reed, K.E., Fleagle, J.G., Leakey, R.E. (Eds.), The paleobiology of
605 *Australopithecus*. Springer, Dordrecht, pp. 7–20. https://doi.org/10.1007/978-94-007-5919-0_2
606
607 Brunet, M., Beauvilain, A., Coppens, Y., Heintz, E., Moutaye, A.H.E., Pilbeam, D., 1995. The first
608 australopithecine 2,500 kilometres west of the Rift Valley (Chad). Nature 378, 273–275.
609 https://doi.org/10.1038/378273a0
610
611 Brunet, M., Beauvilain, A., Coppens, Y., Heintz, E., Moutaye, A.H.E., Pilbeam, D., 1996.
612 *Australopithecus bahrelghazali*, une nouvelle espèce d'Hominidé ancien de la région de Koro Toro
613 (Tchad). C. R. Acad. Sci. Paris 322, 907–913.
614
615 Bruxelles, L., Stratford, D.J., Maire, R., Pickering, T.R., Heaton, J.L., Beaudet, A., Kuman, K.,
616 Crompton, R., Carlson K.J., Jashashvili, T., McClymont, J., Leader, G.M., Clarke, R.J., 2019. A
617 multiscale stratigraphic investigation of the context of StW 573 'Little Foot'and Member 2,
618 Sterkfontein Caves, South Africa. J. Hum. Evol. 133, 78–98.
619 https://doi.org/10.1016/j.jhevol.2019.05.008
620
621 Caley, T., Extier, T., Collins, J. A., Schefuß, E., Dupont, L., Malaizé, B., Rossignol, L., Souron, A.,
622 McClymont, E.L., Jimenez-Espejo, F.J., García-Comas, C., Eynaud, F., Martinez, P., Roche, D.M.,
623 Jorry, S.J., Charlier, K., Wary, M., Gourves, P.-Y., Billy, I., Giraudeau, J., 2018. A two-million-year-

long hydroclimatic context for hominin evolution in southeastern Africa. Nature 560(7716), 76–79. https://doi.org/10.1038/s41586-018-0309-6

Cerling, T.E., Wynn, J.G., Andanje, S.A., Bird, M.I., Korir, D.K., Levin, N.E., Mace, W., Macharia, A.N., Quade, J., Remien, C.H., 2011. Woody cover and hominin environments in the past 6 million years. Nature 476(7358), 51–56. https://doi.org/10.1038/nature10306

Clarke, R.J., Kuman, K., 2019. The skull of StW 573, a 3.67 Ma *Australopithecus prometheus* skeleton from Sterkfontein Caves, South Africa. J. Hum. Evol. 134, 102634. https://doi.org/10.1016/j.jhevol.2019.06.005

Cobos, M.E., Peterson, A.T., Barve, N., Osorio-Olvera, L., 2019. kuenm: an R package for detailed development of ecological niche models using Maxent. PeerJ 7, e6281. https://doi.org/10.7717/peerj.6281

Contoux, C., Dumas, C., Ramstein, G., Jost, A., Dolan, A.M., 2015. Modelling Greenland ice sheet inception and sustainability during the Late Pliocene. Earth Planet. Sci. Lett. 424, 295–305. https://doi.org/10.1016/j.epsl.2015.05.018

Contoux, C., Jost, A., Ramstein, G., Sepulchre, P., Krinner, G., Schuster, M., 2013. Megalake Chad impact on climate and vegetation during the late Pliocene and the mid-Holocene. Clim. Past 9(4), 1417–1430. https://doi.org/10.5194/cp-9-1417-2013

Contoux, C., Ramstein, G., Jost, A., 2012. Modelling the mid-Pliocene Warm Period climate with the IPSL coupled model and its atmospheric component LMDZ5A. Geosci. Model Dev. 5, 903–917. https://doi.org/10.5194/gmd-5-903-2012

Coulthard, T.J., Ramirez, J.A., Barton, N., Rogerson, M., Brücher, T., 2013. Were rivers flowing across the Sahara during the last interglacial? Implications for human migration through Africa. PloS ONE 8(9), e74834. https://doi.org/10.1371/journal.pone.0074834

Curran, S.C., Haile-Selassie, Y., 2016. Paleoecological reconstruction of hominin-bearing middle Pliocene localities at Woranso-Mille, Ethiopia. J. Hum. Evol. 96, 97–112. https://doi.org/10.1016/j.jhevol.2016.04.002

Dart, R.A., 1925. *Australopithecus africanus*: the man-ape of South Africa. Nature 115, 195–199.

Deino, A.L., Scott, G.R., Saylor, B., Alene, M., Angelini, J.D., Haile-Selassie, Y., 2010. 40Ar/39Ar dating, paleomagnetism, and tephrochemistry of Pliocene strata of the hominid-bearing Woranso-Mille area, west-central Afar Rift, Ethiopia. J. Hum. Evol. 58(2), 111–126. https://doi.org/10.1016/j.jhevol.2009.11.001

deMenocal, P.B., 2004. African climate change and faunal evolution during the Pliocene–Pleistocene. Earth Planet. Sci. Lett. 220, 3–24. https://doi.org/10.1016/S0012-821X(04)00003-2

De Schepper, S., Gibbard, P.L., Salzmann, U., Ehlers, J., 2014. A global synthesis of the marine and terrestrial evidence for glaciation during the Pliocene Epoch. Earth-Sci. Rev. 135, 83–102. https://doi.org/10.1016/j.earscirev.2014.04.003

DiMaggio, E.N., Campisano, C.J., Rowan, J., Dupont-Nivet, G., Deino, A.L., Bibi, F., Lewis, M.E., Souron, A., Garello, D., Werdelin, L., Reed, K.E., Arrowsmith, J.R., 2015. Late Pliocene fossiliferous sedimentary record and the environmental context of early *Homo* from Afar, Ethiopia. Science 347(6228), 1355–1359. https://doi.org/10.1126/science.aaa1415

Dufresne, J.-L., Foujols, M.-A., Denvil, S., Caubel, A., Marti, O., Aumont, O., Balkanski, Y., Bekki, S., Bellenger, H., Benshila, R., Bony, S., Bopp, L., Braconnot, P., Brockmann, P., Cadule, P., Cheruy,

680 F., Codron, F., Cozic, A., Cugnet, D., de Noblet, N., Duvel, J.-P., Ethé, C., Fairhead, L., Fichefet, T.,
681 Flavoni, S., Friedlingstein, P., Grandpeix, J.-Y., Guez, L., Guilyardi, E., Hauglustaine, D., Hourdin, F.,
682 Idelkadi, A., Ghattas, J., Joussaume, S., Kageyama, M., Krinner, G., Labetoulle, S., Lahellec, A.,
683 Lefebvre, M.-P., Lefevre, F., Levy, C., Li, Z.X., Lloyd, J., Lott, F., Madec, G., Mancip, M., Marchand,
684 M., Masson, S., Meurdesoif, Y., Mignot, J., Musat, I., Parouty, S., Polcher, J., Rio, C., Schulz, M.,
685 Swingedouw, D., Szopa, S., Talandier, C., Terray, P., Viovy, N., Vuichard, N. 2013. Climate change
686 projections using the IPSL-CM5 Earth System Model: from CMIP3 to CMIP5. Clim. Dyn. 40(9),
687 2123–2165. https://doi.org/10.1007/s00382-012-1636-1
688
689 Elith, J., Graham, C.H., Anderson, R.P., Dudík, M., Ferrier, S., Guisan, A., Hijmans, R.J., Huettmann,
690 F., Leathwick, J.R., Lehmann, A., Li, J., Lohmann, L.G., Loiselle, B.A., Manion, G., Moritz, C.,
691 Nakamura, M., Nakazawa, Y., Overton, J.McC.M., Peterson, A.T., Phillips, S.J., Richardson, K.,
692 Scachetti-Pereira, R., Schapire, R.E., Zimmermann, N. E., 2006. Novel methods improve prediction of
693 species' distributions from occurrence data. Ecography 29(2), 129–151.
694 https://doi.org/10.1111/j.2006.0906-7590.04596.x
695
696 Guisan, A., Thuiller, W., Zimmermann, N.E., 2017. Habitat suitability and distribution models: with
697 applications in R, Cambridge University Press, Cambridge, UK.
698
699 Fara, E., Likius, A., Mackaye, H.T., Vignaud, P., Brunet, M., 2005. Pliocene large-mammal
700 assemblages from northern Chad: sampling and ecological structure. Naturwissenschaften 92, 537–
701 541. https://doi.org/10.1007/s00114-005-0041-6
702
703 Feibel, C.S., 2011. A Geological History of the Turkana Basin. Evol. Anthropol. 20, 206–216.
704 https://doi.org/10.1002/evan.20331
705
706 Fielding, A.H., Bell, J.F., 1997. A review of methods for the assessment of prediction errors in
707 conservation presence/absence models. Environ. Conserv. 24, 38–49.
708 https://doi.org/10.1017/S0376892997000088
709
710 Fleagle, J.G., Rasmussen, D.T., Yirga, S., Bown, T.M., Grine, F.E., 1991. New hominid fossils from
711 Fejej, Southern Ethiopia. J. Hum. Evol. 21, 145–152. https://doi.org/10.1016/0047-2484(91)90005-G
712
713 Foley, R.A., 2013. Comparative Evolutionary Models and the "Australopith Radiations", in: Reed,
714 K.E., Fleagle, J.G., Leakey, R.E. (Eds.), The paleobiology of *Australopithecus*. Springer, Dordrecht ,
715 pp. 163–174. https://doi.org/10.1007/978-94-007-5919-0_10
716
717 Good, S.P., Caylor, K.K., 2011. Climatological determinants of woody cover in Africa. Proc. Natl.
718 Acad. Sci. USA 108(12), 4902–4907. https://doi.org/10.1073/pnas.1013100108
719
720 Granger, D.E., Gibbon, R.J., Kuman, K., Clarke, R.J., Bruxelles, L., Caffee, M.W., 2015. New
721 cosmogenic burial ages for Sterkfontein member 2 *Australopithecus* and member 5 Oldowan. Nature
722 522(7554), 85–88. https://doi.org/10.1038/nature14268
723
724 Haile-Selassie, Y., Deino, A., Saylor, B., Umer, M., Latimer, B., 2007. Preliminary geology and
725 paleontology of new hominid-bearing Pliocene localities in the central Afar region of Ethiopia.
726 Anthropol. Sci. 115, 215–222. https://doi.org/10.1537/ase.070426.
727
728 Haile-Selassie, Y., Gibert, L., Melillo, S.M., Ryan, T.M., Alene, M., Deino, A., Levin, N.E., Scott,
729 G.,.Saylor, B.Z., 2015. New species from Ethiopia further expands Middle Pliocene hominin diversity.
730 Nature 521(7553), 483–488. https://doi.org/10.1038/nature14448
731
732 Haile-Selassie, Y., Melillo, S.M., Vazzana, A., Benazzi, S., Ryan, T.M., 2019. A 3.8-million-year-old
733 hominin cranium from Woranso-Mille, Ethiopia. Nature 573, 214–219. https://doi:10.1038/s41586-
734 019-1513-8
735

736 Haile-Selassie, Y., Saylor, B.Z., Deino, A., Levin, N.E., Alene, M., Latimer, B.M., 2012. A new
737 hominin foot from Ethiopia shows multiple Pliocene bipedal adaptations. Nature 483(7391), 565–569.
738 https://doi.org/10.1038/nature10922
739
740 Harmand, S., Lewis, J.E., Feibel, C.S., Lepre, C.J., Prat, S., Lenoble, A., Harmand, S., Lewis, J.E.,
741 Feibel, C.S., Lepre, C.J., Prat, S., Lenoble, A., Boës, X., Quinn, R.L., Brenet, M., Arroyo, A., Taylor,
742 N., Clément, S., Daver, G., Brugal, J.-P., Leakey, L., Mortlock, R.A., Wright, J.D., Lokorodi, S.,
743 Kirwa, C., Kent, D.V., Roche, H., 2015. 3.3-million-year-old stone tools from Lomekwi 3, West
744 Turkana, Kenya. Nature 521(7552), 310–315. https://doi.org/10.1038/nature14464
745
746 Haywood, A.M., Dowsett, H.J., Otto-Bliesner, B., Chandler, M.A., Dolan, A.M., Hill, D.J., Robinson,
747 M.M., Rosenbloom N., Salzmann, U., Sohl, L.E., 2010. Pliocene model intercomparison project
748 (PlioMIP): experimental design and boundary conditions (experiment 1). Geosci. Model Dev. 3(1),
749 227–242. https://doi.org/10.5194/gmd-3-227-2010
750
751 Haywood, A.M., Tindall, J.C., Dowsett, H.J., Dolan, A.M., Foley, K.M., Hunter, S.J., Hill, D.J., Chan,
752 W.-L., Abe-Ouchi, A., Stepanek, C., Lohmann, G., Chandan, D., Peltier, W.R., Tan, N., Contoux, C.,
753 Ramstein, G., Li, X., Zhang, Z., Guo, C., Nisancioglu, K.H., Zhang, Q., Li, Q., Kamae, Y., Chandler,
754 M.A., Sohl, L.E., Otto-Bliesner, B.L., Feng, R., Brady, E.C., von der Heydt, A.S., Baatsen, M.L.J.,
755 Lunt, D.J., 2020. The Pliocene Model Intercomparison Project Phase 2: large-scale climate features
756 and climate sensitivity. Clim. Past 16, 2095–2123. https://doi.org/10.5194/cp-16-2095-2020
757
758 Hély, C., Braconnot, P., Watrin, J., Zheng, W., 2009. Climate and vegetation: simulating the African
759 humid period. C. R. Geoscience 341, 671–688. https://doi.org/10.1016/j.crte.2009.07.002.
760
761 Hernandez, P.A., Graham, C.H., Master, L.L., Albert, D.L., 2006. The effect of sample size and
762 species characteristics on performance of different species distribution modeling methods. Ecography
763 29, 773–785. https://doi.org/10.1111/j.0906-7590.2006.04700.x
764
765 Herries, A.I., Pickering, R., Adams, J.W., Curnoe, D., Warr, G., Latham, A.G., Shaw, J., 2013. A
766 multi-disciplinary perspective on the age of *Australopithecus* in southern Africa, in: Reed, K.E.,
767 Fleagle, J.G., Leakey, R.E. (Eds.), The paleobiology of *Australopithecus*. Springer, Dordrecht, pp. 21–
768 40. https://doi.org/10.1007/978-94-007-5919-0_3
769
770 Joannes-Boyau, R., Adams, J.W., Austin, C., Arora, M., Moffat, I., Herries, A.I.R., Tonge, M.P.,
771 Benazzi, S., Evans, A.R., Kullmer, O., Wroe, S., Dosseto, A., Fiorenza, L., 2019. Elemental signatures
772 of *Australopithecus africanus* teeth reveal seasonal dietary stress. Nature 572(7767), 112–115.
773 https://doi.org/10.1038/s41586-019-1370-5
774
775 Joordens, J.C.A., Feibel, C.S., Vonhof, H.B., Schulp, A.S., Kroon, D., 2019. Relevance of the eastern
776 African coastal forest for early hominin biogeography. J. Hum. Evol. 131, 176–202.
777 https://doi.org/10.1016/j.jhevol.2019.03.012
778
779 Kageyama, M., Braconnot, P., Bopp, L., Caubel, A., Foujols, M.-A., Guilyardi, E., Khodri, M., Lloyd,
780 J., Lombard, F., Mariotti, V., Marti, O., Roy, T., Woillez, M.-N. 2013. Mid-Holocene and Last Glacial
781 Maximum climate simulations with the IPSL model—part I: comparing IPSL_CM5A to IPSL_CM4.
782 Clim. Dyn. 40(9-10), 2447–2468. https://doi.org/10.1007/s00382-012-1488-8
783
784 Kaplan, J.O., Bigelow, N.H., Prentice, I.C., Harrison, S.P., Bartlein, P.J., Christensen, T.R., Cramer,
785 W., Matveyeva, N.V., McGuire, A.D., Murray, D.F., Razzhivin, V.Y., Smith, B., Walker, D.A.,
786 Anderson, P.M., Andreev, A.A., Brubaker, L.B., Edwards, M.E., Lozhkin, A.V., 2003. Climate
787 change and Arctic ecosystems: 2. Modeling, paleodata-model comparisons, and future projections. J.
788 Geophys. Res. Atmos. 108(D19), 8171. https://doi.org/10.1029/2002JD002559
789
790 Kappelman, J., Swisher III, C.C., Fleagle, J.G., Yirga, S., Bown, T.M., Feseha, M., 1996. Age of
791 *Australopithecus afarensis* from Fejej, Ethiopia. J. Hum. Evol. 30(2), 139–146.

Kingdon, J., 2003. Lowly origin: where, when, and why our ancestors first stood up. Princeton University Press, Princeton. https://doi.org/10.1073/pnas.1807912115

Kullmer, O., Sandrock, O., Viola, T.B., Hujer, W., Said, H., Seidler, H., 2008. Suids, elephantoids, paleochronology, and paleoecology of the Pliocene hominid site Galili, Somali Region, Ethiopia. Palaios 23(7), 452–464. https://doi.org/10.2110/palo.2007.p07-028r

Krinner, G., Flanner, M.G., 2018. Striking stationarity of large-scale climate model bias patterns under strong climate change. Proc. Natl. Acad. Sci. USA 115(38), 9462–9466.

Kröpelin, S., Verschuren, D., Lézine, A.M., Eggermont, H., Cocquyt, C., Francus, P., Cazet, J.-P., Fagot, M., Rumes, B., Russell, J.M., Darius, F., Conley, D.J., Schuster, M., von Suchodoletz, H., Engstrom, D.R., 2008. Climate-driven ecosystem succession in the Sahara: the past 6000 years. Science 320(5877), 765–768. https://doi.org/10.1126/science.1154913

Larrasoaña, J.C., Roberts, A.P., Rohling, E.J., 2013. Dynamics of green Sahara periods and their role in hominin evolution. PLoS ONE 8, e76514. https://doi.org/10.1371/journal.pone.0076514

Laskar, J., Robutel, P., Joutel, F., Gastineau, M., Correia, A.C.M., Levrard, B., 2004. A long-term numerical solution for the insolation quantities of the Earth. Astron. Astrophys. 428(1), 261–285. https://doi.org/10.1051/0004-6361:20041335

Leakey, M.G., Feibel, C.S., McDougall, I., Ward, C., Walker, A., 1998. New specimens and confirmation of an early age for *Australopithecus anamensis*. Nature 393, 62–66. https://doi.org/10.1038/29972

Leakey, M.G., Spoor, F., Brown, F.H., Gathogo, P.N., Kiarie, C., Leakey, L.N., McDougall, I., 2001. New hominin genus from eastern Africa shows diverse middle Pliocene lineages. Nature 410(6827), 433–440. https://doi.org/10.1038/35068500

Leakey, M.G., Walker, A.C., 2003. The Lothagam hominids. In: Leakey, M.G., Harris, J.M. (Eds.), Lothagam. Columbia University Press, New York, pp. 249–258. https://doi.org/10.7312/leak11870

Lebatard, A.-E., Bourlès, D.L., Duringer, P., Jolivet, M., Braucher, R., Carcaillet, J., Schuster, M., Arnaud, N., Monié, P., Lihoreau, F., Likius, A., Mackaye, H.T., Vignaud, P., Brunet, M., 2008. Cosmogenic nuclide dating of *Sahelanthropus tchadensis* and *Australopithecus bahrelghazali*: Mio-Pliocene hominids from Chad. Proc. Natl. Acad. Sci. USA 105(9), 3226–3231. https://doi.org/10.1073/pnas.0708015105

Lee-Thorp, J., Likius, A., Mackaye, H.T., Vignaud, P., Sponheimer, M., Brunet, M., 2012. Isotopic evidence for an early shift to C4 resources by Pliocene hominins in Chad. Proc. Natl. Acad. Sci. USA 109(50), 20369–20372. https://doi.org/10.1073/pnas.1204209109

Le Fur, S., Fara, E., Mackaye, H.T., Vignaud, P., Brunet, M., 2009. The mammal assemblage of the hominid site TM266 (Late Miocene, Chad Basin): ecological structure and paleoenvironmental implications. Naturwissenschaften, 96, 565–574. https://doi.org/10.1007/s00114-008-0504-7

Levin, N.E., Simpson, S.W., Quade, J., Cerling, T.E., Frost, S.R., 2008. Herbivore enamel carbon isotopic composition and the environmental context of *Ardipithecus* at Gona, Ethiopia. In: Quade, J., Wynn, J.G. (Eds.), The geology of early humans in the Horn of Africa. Geological Society of America, pp. 215–234. https://doi.org/*10.1130/2008.2446(10)*

Liddy, H.M., Feakins, S.J., Tierney, J.E., 2016. Cooling and drying in northeast Africa across the Pliocene. Earth Planet. Sci. Lett. 449, 430–438. https://doi.org/10.1016/j.epsl.2016.05.005

Lieberman, D.E., 2015. Human locomotion and heat loss: an evolutionary perspective. Compr. Physiol. 5, 99–117. https://doi.org/10.1002/cphy.c140011

Lisiecki, L.E., Raymo, M.E., 2005. A Pliocene-Pleistocene stack of 57 globally distributed benthic $\delta^{18}O$ records. Paleoceanography 20(1), PA1003. https://doi.org/10.1029/2004PA001071

Marston, C.G., Wilkinson, D.M., Reynolds, S.C., Louys, J., O'Regan, H.J., 2019. Water availability is a principal driver of large-scale land cover spatial heterogeneity in sub-Saharan savannahs. Landsc. Ecol. 34(1), 131–145. https://doi.org/10.1007/s10980-018-0750-9

Mbua, E., Kusaka, S., Kunimatsu, Y., Geraads, D., Sawada, Y., Brown, F.H., Sakai, T., Boisserie, J.-R., Saneyoshi, M., Omuombo, C., Muteti, S., Hirata, T., Hayashida, A., Iwano, H., Danhara, T., Bobe, R., Jicha, B., Nakatsukasa, M., 2016. Kantis: A new *Australopithecus* site on the shoulders of the Rift Valley near Nairobi, Kenya. J. Hum. Evol. 94, 28–44. https://doi.org/10.1016/j.jhevol.2016.01.006

McKee, J.K., Kuykendall, K.L., 2016. The Dart Deposits of the Buxton Limeworks, Taung, South Africa, and the context of the Taung *Australopithecus* fossil. J. Vert. Paleontol. 36, e1054937. https://doi.org/10.1080/02724634.2015.1054937

Merow, C., Smith, M.J., Silander, J.A., 2013. A practical guide to MaxEnt for modeling species' distributions: what it does, and why inputs and settings matter. Ecography 36, 1058–1069. https://doi.org/10.1111/j.1600-0587.2013.07872.x

New, M., Lister, D., Hulme, M., Makin, I., 2002. A high-resolution data set of surface climate over global land areas. Clim. Res. 21, 1–25. https://doi:10.3354/cr021001

Novello, A., Barboni, D., Sylvestre, F., Lebatard, A.-E., Paillès, C., Bourlès, D.L., Likius, A., Mackaye, H.T., Vignaud, P., Brunet, M., 2017. Phytoliths indicate significant arboreal cover at *Sahelanthropus* type locality TM266 in northern Chad and a decrease in later sites. J. Hum. Evol. 106, 66–83. https://doi.org/10.1016/j.jhevol.2017.01.009

Owens, H.L., Campbell, L.P., Dornak, L.L., Saupe, E.E., Barve, N., Soberón, J., Ingenloff, K., Lira-Noriega, A., Hensz, C.M., Myers, C.E., Peterson, A.T., 2013. Constraints on interpretation of ecological niche models by limited environmental ranges on calibration areas. Ecol. Model. 263, 10–18. https://doi.org/10.1016/j.ecolmodel.2013.04.011

Paillard, D., Labeyrie, L.D., Yiou, P., 1996. AnalySeries 1.0: a Macintosh software for the analysis of geophysical time-series. Eos 77, 379.

Passey, B.H., Levin, N.E., Cerling, T.E., Brown, F.H., Eiler, J.M., 2010. High-temperature environments of human evolution in East Africa based on bond ordering in paleosol carbonates. Proc. Natl. Acad. Sci. USA 107, 11245–11249. https://doi.org/10.1073/pnas.1001824107

Pearson, R.G., Raxworthy, C.J., Nakamura, M., Peterson, A.T., 2006. Predicting species distributions from small numbers of occurrence records: a test case using cryptic geckos in Madagascar. J. Biogeogr. 34, 102–117. https://doi.org/10.1111/j.1365-2699.2006.01594.x

Peel, M.C., Finlayson, B.L., McMahon, T.A., 2007. Updated world map of the Köppen-Geiger climate classification. Hydrol. Earth Syst. Sci. 11(5), 1633–1644. https://doi.org/10.5194/hess-11-1633-2007

Peterson, A.T., Cobos, M.E., Jiménez-García, D., 2018. Major challenges for correlational ecological niche model projections to future climate conditions. Ann. N. Y. Acad. Sci. 1429(1), 66–77. https://doi.org/10.1111/nyas.13873

902 Peterson, A.T., Papeş, M., Eaton, M., 2007. Transferability and model evaluation in ecological niche
903 modeling: A comparison of GARP and Maxent. Ecography, 30(4), 550–560.
904 https://doi.org/10.1111/j.0906-7590.2007.05102.x
905
906 Peterson, A.T., Papeş, M., Soberón, J., 2008. Rethinking receiver operating characteristic analysis
907 applications in ecological niche modeling. Ecol. Model. 213, 63–72.
908 https://doi.org/10.1016/j.ecolmodel.2007.11.008.
909
910 Peterson, A.T., Soberón, J., Pearson, R.G., Anderson, R.P., Martínez-Meyer, E., Nakamura, M.,
911 Araújo, M.B., 2011. Ecological niches and geographic distributions (MPB-49). Princeton University
912 Press, Princeton. https://doi.org/10.1515/9781400840670
913
914 Phillips, S.J., Anderson, R.P., Dudík, M., Schapire, R.E., Blair, M.E., 2017. Opening the black box: an
915 open-source release of Maxent. Ecography 40, 887–893. https://doi: 10.1111/ecog.03049
916
917 Phillips, S.J., Anderson, R.P., Schapire, R.E., 2006. Maximum entropy modeling of species
918 geographic distributions. Ecol. Model. 190, 231–259. https://doi.org/10.1016/j.ecolmodel.2005.03.026
919
920 Phillips, S.J., Dudík, M., 2008. Modeling of species distributions with Maxent: new extensions and a
921 comprehensive evaluation. Ecography 31, 161–175. https://doi.org/10.1111/j.0906-7590.2008.5203.x
922
923 Quade, J., Dente, E., Armon, M., Dor, Y.B., Morin, E., Adam, O., Enzel, Y., 2018. Megalakes in the
924 Sahara? A review. Quat. Res. 90(2), 253–275. https://doi.org/10.1017/qua.2018.46
925
926 Quinn, R.L., 2019. Isotopic equifinality and rethinking the diet of *Australopithecus anamensis*. Am. J.
927 Phys. Anthropol. 169, 403–421. https://doi.org/10.1002/ajpa.23846
928
929 Quinn, R.L., Lepre, C.J., 2020. Revisiting the pedogenic carbonate isotopes and paleoenvironmental
930 interpretation of Kanapoi. J. Hum. Evol. 140, 102549. https://doi:10.1016/j.jhevol.2018.11.005
931
932 Raes, N., ter Steege, H., 2007. A null-model for significance testing of presence-only species
933 distribution models. Ecography 30, 727–736. https://doi.org/10.1111/j.2007.0906-7590.05041.x
934
935 Reed, K.E., 1997. Early hominid evolution and ecological change through the African Plio-
936 Pleistocene. J. Hum. Evol. 32, 289–322. https://doi.org/10.1006/jhev.1996.0106
937
938 Renne, P.R., WoldeGabriel, G., Hart, W.K., Heiken, G., White, T.D., 1999. Chronostratigraphy of the
939 Miocene–Pliocene Sagantole Formation, Middle Awash Valley, Afar rift, Ethiopia. Geol. Soc. Am.
940 Bull. 111, 869–885. https://doi.org/10.1130/0016-7606(1999)111%3C0869:COTMPS%3E2.3.CO;2
941
942 Robinson, J.R., Rowan, J., Campisano, C.J., Wynn, J.G., Reed, K.E., 2017. Late Pliocene
943 environmental change during the transition from *Australopithecus* to *Homo*. Nat. Ecol. Evol. 1, 0159.
944 https://doi.org/10.1038/s41559-017-0159
945
946 Sahnouni, M., Parés, J.M., Duval, M., Cáceres, I., Harichane, Z., van der Made, J., Pérez-González,
947 A., Abdessadok, S., Kandi, N., Derradji, A., Medig, M., Boulaghraif, K., Semaw, S. 2018. 1.9-million-
948 and 2.4-million-year-old artifacts and stone tool–cutmarked bones from Ain Boucherit, Algeria.
949 Science 362(6420), 1297–1301. https://doi.org/10.1126/science.aau0008
950
951 Salzmann, U., Haywood, A.M., Lunt, D.J., Valdes, P.J., Hill, D.J., 2008. A new global biome
952 reconstruction and data-model comparison for the Middle Pliocene. Glob. Ecol. Biogeogr. 17, 432–
953 447. https://doi.org/10.1111/j.1466-8238.2008.00381.x
954
955 Saylor, B.Z., Gibert, L., Deino, A., Alene, M., Levin, N.E., Melillo, S.M., Peaple, M.D., Feakins, S.J.,
956 Bourel, B., Barboni, D., Novello, A., Sylvestre, F., Mertzman, S.A., Haile-Selassie, Y., 2019. Age and

context of mid-Pliocene hominin cranium from Woranso-Mille, Ethiopia. Nature, 573(7773), 220–224. https://doi.org/10.1038/s41586-019-1514-7

Schuster, M., Duringer, P., Ghienne, J.-F., Roquin, C., Sepulchre, P., Moussa, A., Lebatard, A.-E., Mackaye, H.T., Likius, A., Vignaud, P., Brunet, M., 2009. Chad Basin: paleoenvironments of the Sahara since the Late Miocene. C. R. Geoscience 341(8-9), 603–611. https://doi.org/10.1016/j.crte.2009.04.001

Senut, B., 2020. *Orrorin tugenensis* et les origines de l'homme: une synthèse. Bull. Acad. Nat. Méd. 204(3), 258–267. https://doi.org/10.1016/j.banm.2019.12.018

Shcheglovitova, M., Anderson, R.P., 2013. Estimating optimal complexity for ecological niche models: A jackknife approach for species with small sample sizes. Ecol. Model. 269, 9–17. https://doi.org/10.1016/j.ecolmodel.2013.08.011

Skonieczny, C., Paillou, P., Bory, A., Bayon, G., Biscara, L., Crosta, X., Eynaud, F., Malaizé, B., Revel, M., Aleman, N., Barusseau J.-P., Vernet, R., Lopez, S., Grousset, F. 2015. African humid periods triggered the reactivation of a large river system in Western Sahara. Nat. commun. 6(1), 1–6. https://doi.org/10.1038/ncomms9751

Sponheimer, M., 2013. Some ruminations on australopith diets, in: Reed, K.E., Fleagle, J.G., Leakey, R.E. (Eds.), The paleobiology of *Asustralopithecus*. Springer, Dordrecht, pp. 225–233. https://doi.org/10.1007/978-94-007-5919-0_15

Su, D.F., Croft, D.A., 2018. Making sense of the evidence: synthesizing paleoecological data, in: Croft, D.A., Su, D.F., Simpson, S.W. (Eds.), Methods in paleoecology. Springer International Publishing, pp. 395–404. https://doi.org/10.1007/978-3-319-94265-0_18

Su, D.F., Harrison, T., 2008. Ecological implications of the relative rarity of fossil hominins at Laetoli. J. Hum. Evol. 55, 672–681. https://doi.org/10.1016/j.jhevol.2008.07.003

Sussman, R.W., Hart, D., 2015. Modeling the past: the primatological approach, in: Henke, W., Tattersall, I. (Eds.), Handbook of paleoanthropology. Springer, Berlin, Heidelberg, pp. 791–815.

Taieb, M., Coppens, Y., Johanson, C., Bonnefille, R., 1975. Hominidés de l'Afar central, Ethiopie (Site d'Hadar, campagne 1973). Bull. Mém. Soc. Anthropol. Paris 2, 117–124.

Tan, N., Contoux, C., Ramstein, G., Sun, Y., Dumas, C., Sepulchre, P., Guo, Z., 2020. Modeling a modern-like pCO_2 warm period (Marine Isotope Stage KM5c) with two versions of an Institut Pierre Simon Laplace atmosphere–ocean coupled general circulation model. Clim. Past 16, 1–16. https://doi.org/10.5194/cp-16-1-2020

Tan, N., Ladant, J.B., Ramstein, G., Dumas, C., Bachem, P., Jansen, E., 2018. Dynamic Greenland ice sheet driven by pCO_2 variations across the Pliocene Pleistocene transition. Nat. Commun. 9, 4755. https://doi.org/10.1038/s41467-018-07206-w

Tan, N., Ramstein, G., Dumas, C., Contoux, C., Ladant, J.B., Sepulchre, P., Zhang, Z., De Schepper, S., 2017. Exploring the MIS M2 glaciation occurring during a warm and high atmospheric CO2 Pliocene background climate. Earth Planet. Sci. Lett. 472, 266–276. https://doi.org/10.1016/j.epsl.2017.04.050

Uno, K.T., Polissar, P.J., Jackson, K.E., deMenocal, P.B., 2016. Neogene biomarker record of vegetation change in eastern Africa. Proc. Natl. Acad. Sci. USA 113, 6355–6363. https://doi.org/10.1073/pnas.1521267113

Vallé, F., Dupont, L.M., Leroy, S.A.G., Schefuß, E., Wefer, G., 2014. Pliocene environmental change in West Africa and the onset of strong NE trade winds (ODP Sites 659 and 658). Palaeogeogr. Palaeoclimatol. Palaeoecol. 414, 403–414. https://doi.org/10.1016/j.palaeo.2014.09.023

VanDerWal, J., Shoo, L.P., Graham, C., Williams, S.E., 2009. Selecting pseudo-absence data for presence-only distribution modeling: how far should you stray from what you know? Ecol. Model. 220(4), 589–594. https://doi.org/10.1016/j.ecolmodel.2008.11.010

Vignaud, P., Duringer, P., Mackaye, H.T., Likius, A., Blondel, C., Boisserie, J.-R., Bonis, L. de, Eisenmann, V., Etienne, M.-E., Geraads, D., Guy, F., Lehmann, T., Lihoreau, F., Lopez-Martinez, N., Mourer-Chauviré, C., Otero, O., Rage, J.-C., Schuster, M., Viriot, L., Zazzo, A., Brunet, M., 2002. Geology and palaeontology of the Upper Miocene Toros-Menalla hominid locality, Chad. Nature, 418(6894), 152–155. https://doi.org/10.1038/nature00880

Ward, C.V., Manthi, F.K., Plavcan, J.M., 2013. New fossils of *Australopithecus anamensis* from Kanapoi, West Turkana, Kenya (2003–2008). J. Hum. Evol. 65, 501–524. https://doi.org/10.1016/j.jhevol.2013.05.006

Warren, D.L., Seifert S.N., 2011. Ecological niche modeling in Maxent: the importance of model complexity and the performance of model selection criteria. Ecol. Appl. 21, 335–342. https://doi.org/10.1890/10-1171.1

White, T.D., Asfaw, B., Beyene, Y., Haile-Selassie, Y., Lovejoy, C.O., Suwa, G., WoldeGabriel, G., 2009. *Ardipithecus ramidus* and the paleobiology of early hominids. Science 326(5949), 64–86. https://doi.org/10.1126/science.1175802

White, T.D., Hart, W.K., Walter, R.C., WoldeGabriel, G., Heinzelin, J. de, Clark, J.D., Asfaw, B., Vrba, E., 1993. New discoveries of *Australopithecus* at Maka in Ethiopia. Nature 366(6452), 261–265. https://doi.org/10.1038/366261a0

White, T.D., Howell, F.C., Gilbert, H., 2006b. The earliest *Metridiochoerus* (Artiodactyla: Suidae) from the Usno Formation, Ethiopia. Trans. R. Soc. S. Afr. 61, 75–79. https://doi.org/10.1080/00359190609519955

White, T.D., Suwa, G., Asfaw, B., 1994. *Australopithecus ramidus*, a new species of early hominid from Aramis, Ethiopia. Nature 371, 306–312. https://doi.org/10.1038/371306a0

White, T.D., WoldeGabriel, G., Asfaw, B., Ambrose, S., Beyene, Y., Bernor, R.L., Boisserie, J.-R., Currie, B.,Gilbert, H., Haile-Selassie, Y., Hart, W.K., Hlusko, L.J., Howell, F.C., Kono, R.T., Lehmann, T., Louchart, A., Lovejoy, C.O., Renne, P.R., Saegusa, H., Vrba, E.S., Wesselman, H., Suwa, G., 2006a. Asa Issie, Aramis and the origin of *Australopithecus*. Nature 440(7086), 883–889. https://doi.org/10.1038/nature04629

WoldeGabriel, G., Ambrose, S.H., Barboni, D., Bonnefille, R., Bremond, L., Currie, B., DeGusta, D., Hart, W.K., Murray, A.M., Renne, P.R., Jolly-Saad, M.C., Stewart, K.M., White, T.D. 2009. The geological, isotopic, botanical, invertebrate, and lower vertebrate surroundings of *Ardipithecus ramidus*. Science 326(5949), 65–65e5. https://doi.org/10.1126/science.1175817

Wynn, J.G., Reed, K.E., Sponheimer, M., Kimbel, W.H., Alemseged, Z., Bedaso, Z.K., Campisano, C. J., 2016. Dietary flexibility of *Australopithecus afarensis* in the face of paleoecological change during the middle Pliocene: Faunal evidence from Hadar, Ethiopia. J. Hum. Evol. 99, 93–106. https://doi.org/10.1016/j.jhevol.2016.08.002

Zhang, R., Yan, Q., Zhang, Z.S., Jiang, D., Otto-Bliesner, B.L., Haywood, A.M., Hill, D.J., Dolan, A.M., Stepanek, C., Lohmann, G., Contoux, C., Bragg, F., Chan, W.-L., Chandler, M.A., Jost, A., Kamae, Y., Abe-Ouchi, A., Ramstein, G., Rosenbloom, N.A., Sohl, L., Ueda, H., 2013. Mid-Pliocene

East Asian monsoon climate simulated in the PlioMIP. Clim. Past 9(5), 2085–2099. https://doi.org/10.5194/cp-9-2085-2013

Zhang, Z., Li, X., Guo, C., Otterå, O.H., Nisancioglu, K.H., Tan, N., Contoux, C., Ramstein, G., Feng, R., Otto-Bliesner, B.L., Brady, E., Chandan, D., Peltier, W.R., Baatsen, M.L.J., von der Heydt, A.S., Weiffenbach, J.E., Stepanek, C., Lohmann, G., Zhang, Q., Li, Q., Chandler, M.A., Sohl, L.E., Haywood, A.M., Hunter, S.J., Tindall, J.C., Williams, C., Lunt, D.J., Chan, W.-L., Abe-Ouchi, A., 2021. Mid-Pliocene Atlantic Meridional Overturning Circulation simulated in PlioMIP2. Clim. Past 17, 529–543. https://doi.org/10.5194/cp-17-529-2021

Zhang, Z., Ramstein, G., Schuster, M., Li, C., Contoux, C., Yan, Q., 2014. Aridification of the Sahara Desert caused by Tethys Sea shrinkage during the Late Miocene. Nature 513(7518), 401–404. https://doi.org/10.1038/nature13705

Climate-inferred distribution of mid-to-late Pliocene hominins

Corentin Gibert, Anaïs Vignoles, Camille Contoux, William E. Banks, Doris Barboni, Jean-Renaud Boisserie, Olivier Chavasseau, Frédéric Fluteau, Franck Guy, Camille Noûs, Olga Otero, Pierre Sepulchre, Antoine Souron, Gilles Ramstein

Appendix 1

Supplementary Figures 1 to 8

Supplementary Table 1

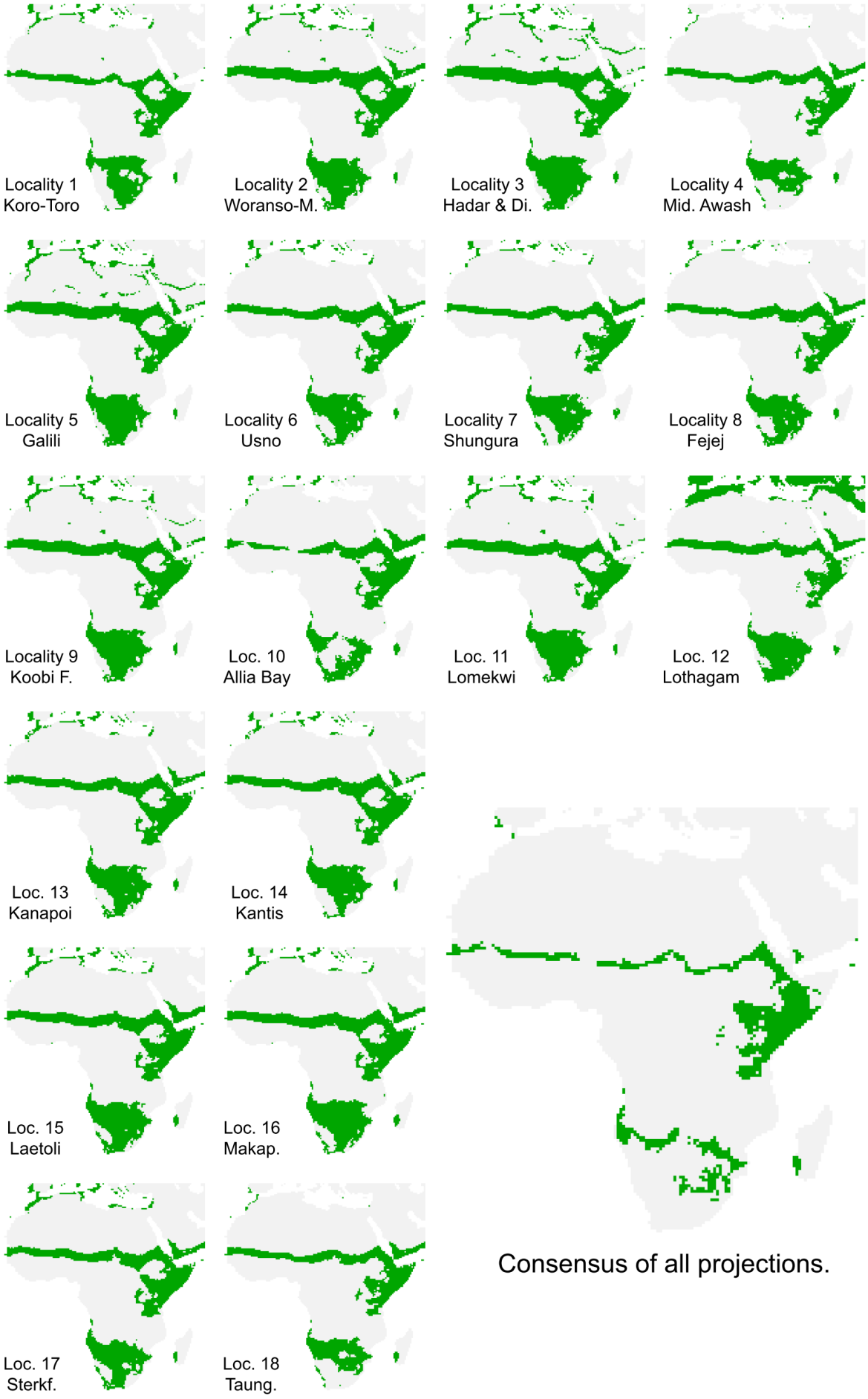

Supplementary Figure 1. Binary map (green for suitable areas) for the 18 jackknife kuenm final models. Named locality is removed, number refers to Table 1. Map in the bottom right is the consensus map of the 18 final models.

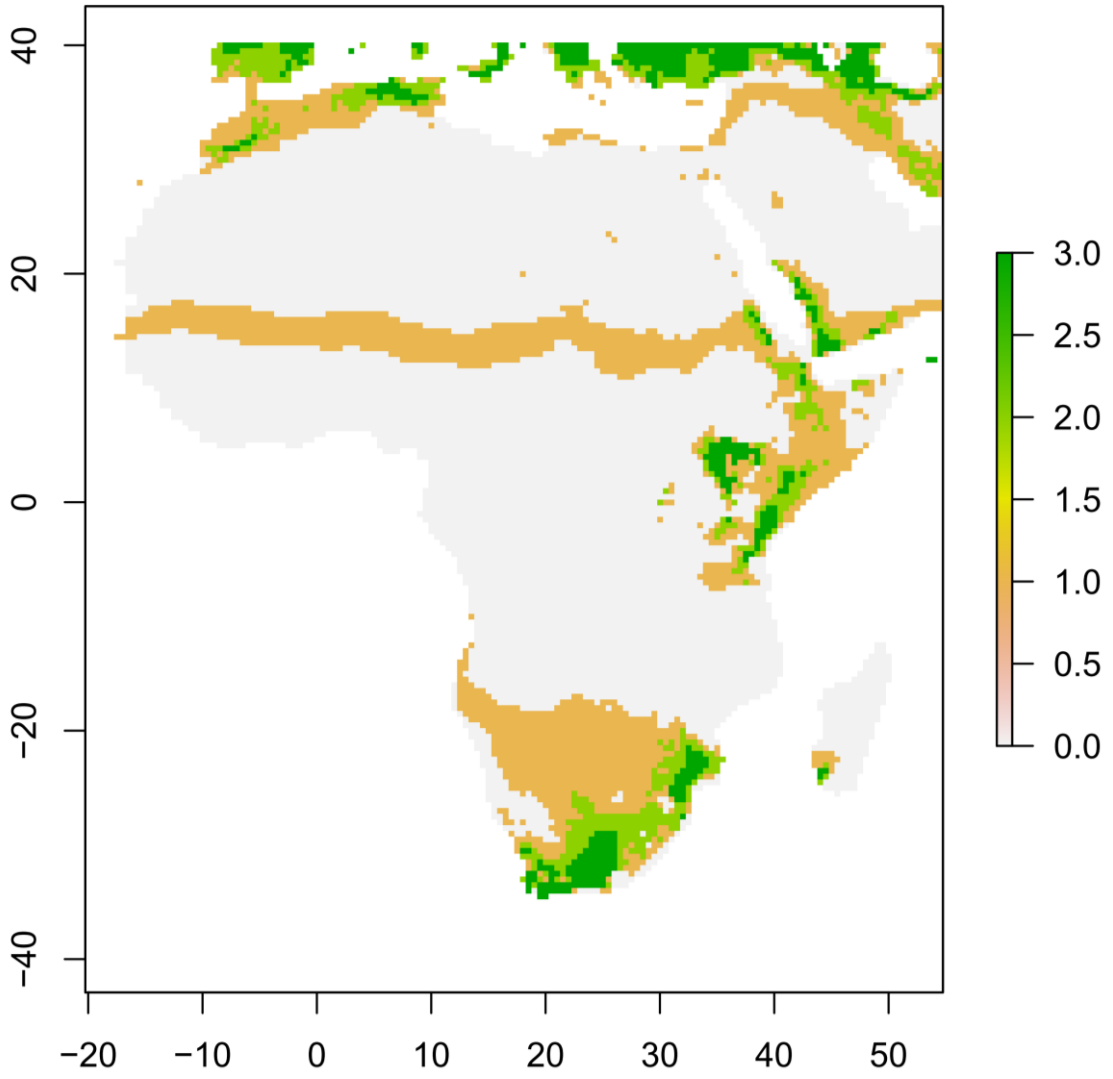

Supplementary Figure 2. Sensitivity test on temporal window of sampling. Au. *anamensis*, Au. *prometheus* and Au. *africanus* are removed resulting in the removal of the three localities from southern Africa. HSM obtained with KUENM and Maxent algorithms. Climatic layers are Pliocene 'mean' climate.

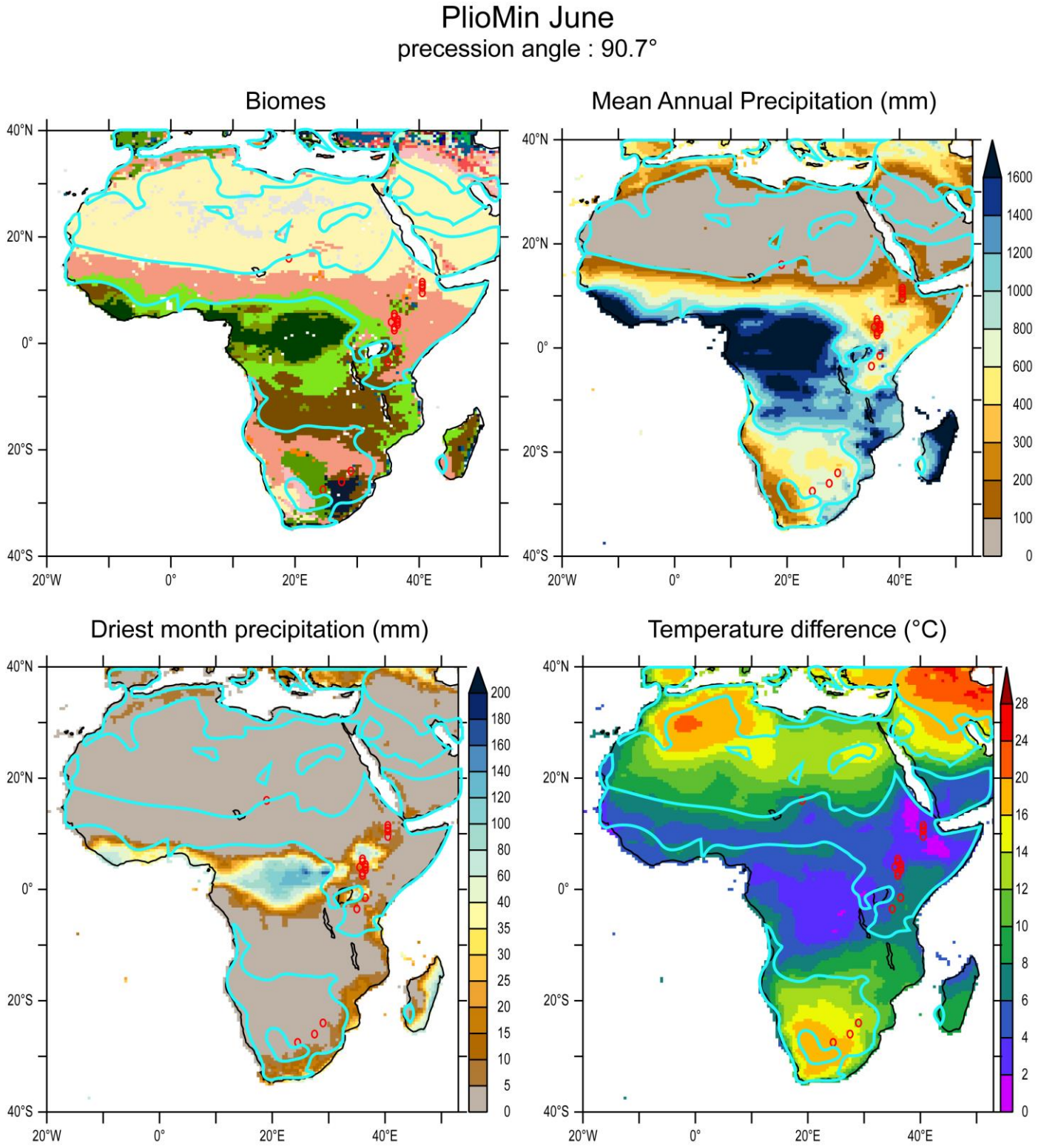

Supplementary Figure 3. Biomes, Mean annual precipitation (MAP), driest month precipitation (DMP), temperature difference between the coldest and warmest months (DT). Areas suitable for hominins from figure 4 PlioMin June final model are marked by contours.

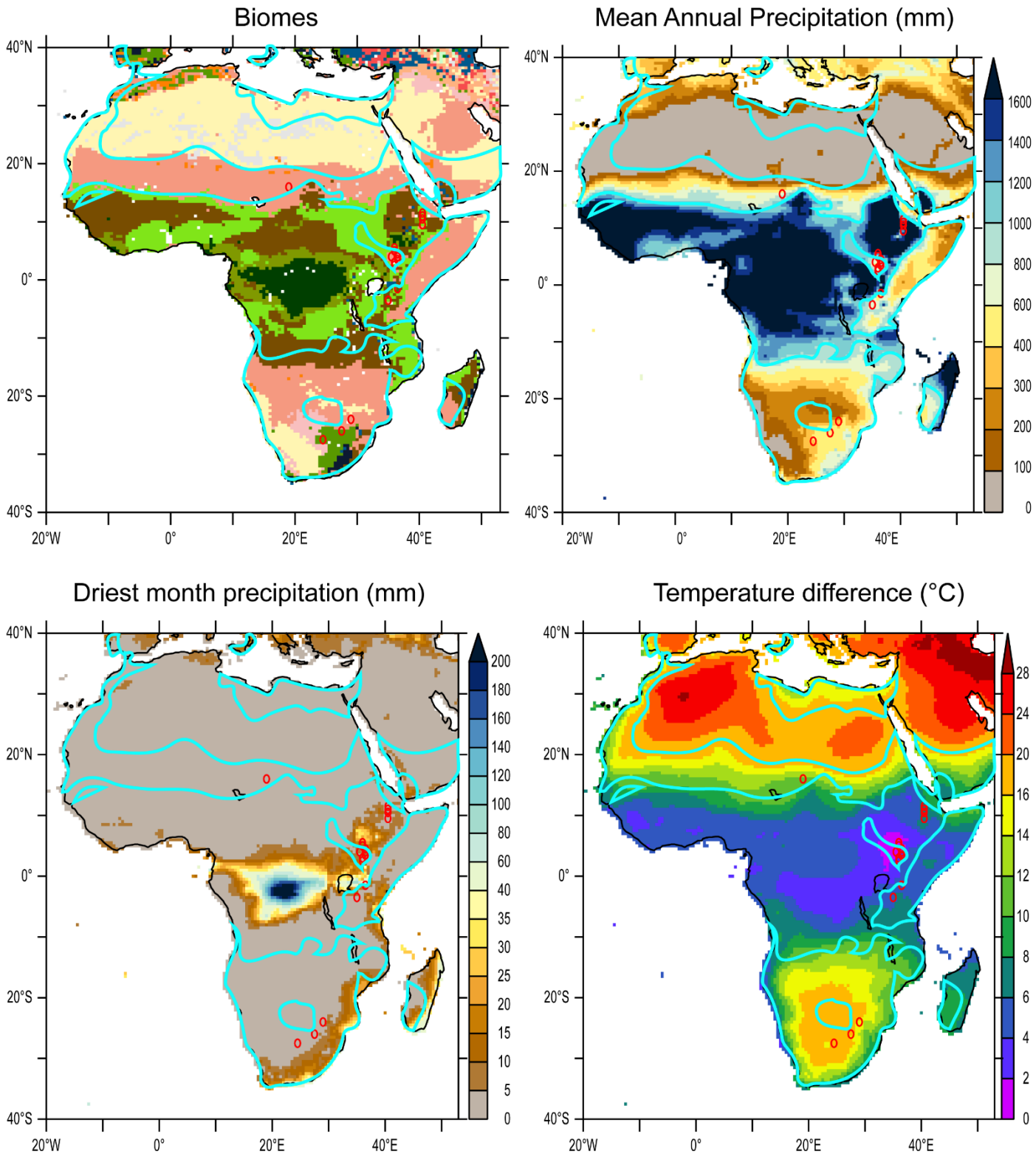

Supplementary Figure 4. Biomes, Mean annual precipitation (MAP), driest month precipitation (DMP), temperature difference between the coldest and warmest months (DT). Areas suitable for hominins from figure 4 PlioMax September final model are marked by contours.

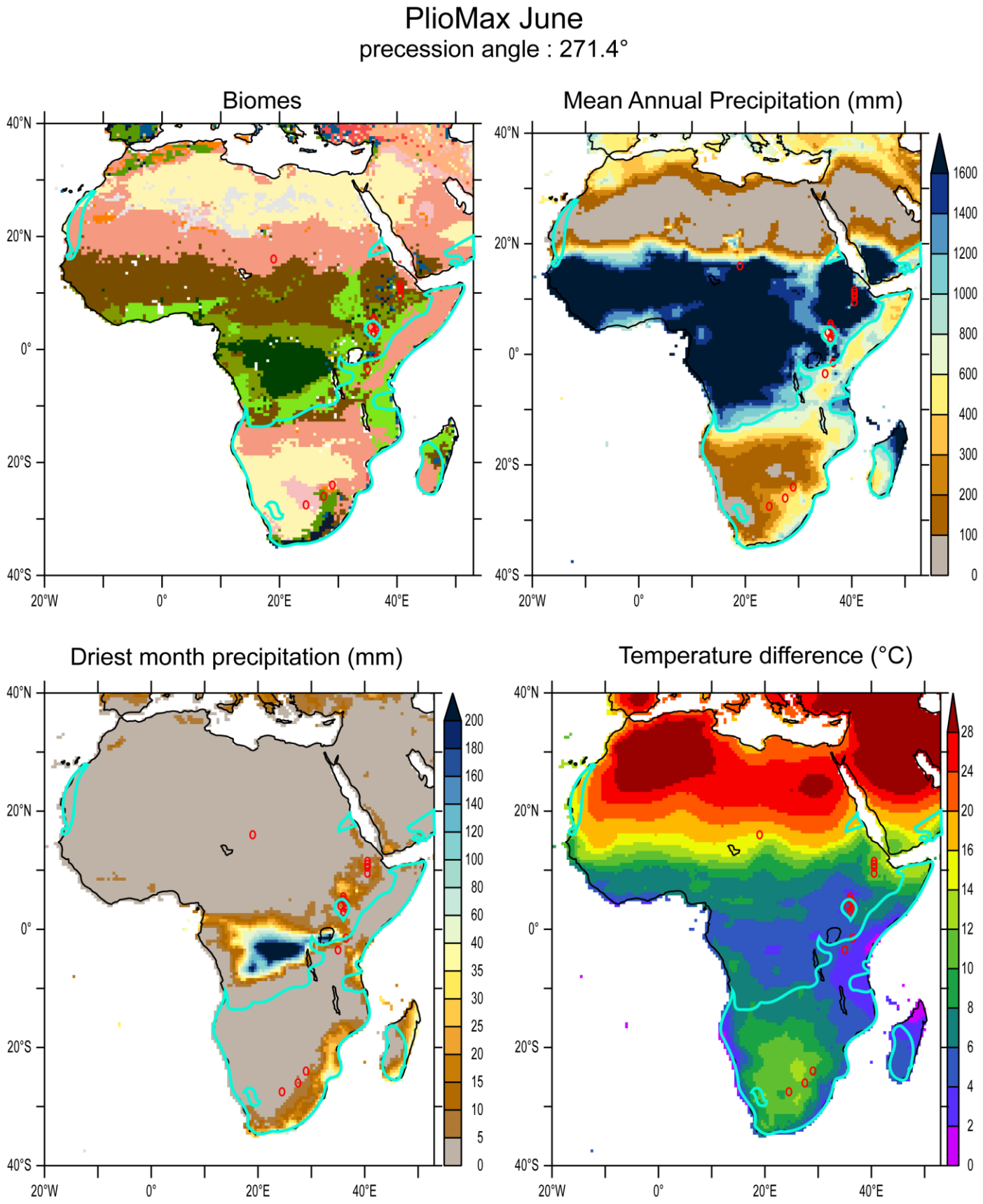

Supplementary Figure 5. Biomes, Mean annual precipitation (MAP), driest month precipitation (DMP), temperature difference between the coldest and warmest months (DT). Areas suitable for hominins from figure 4 PlioMax June final model are marked by contours.

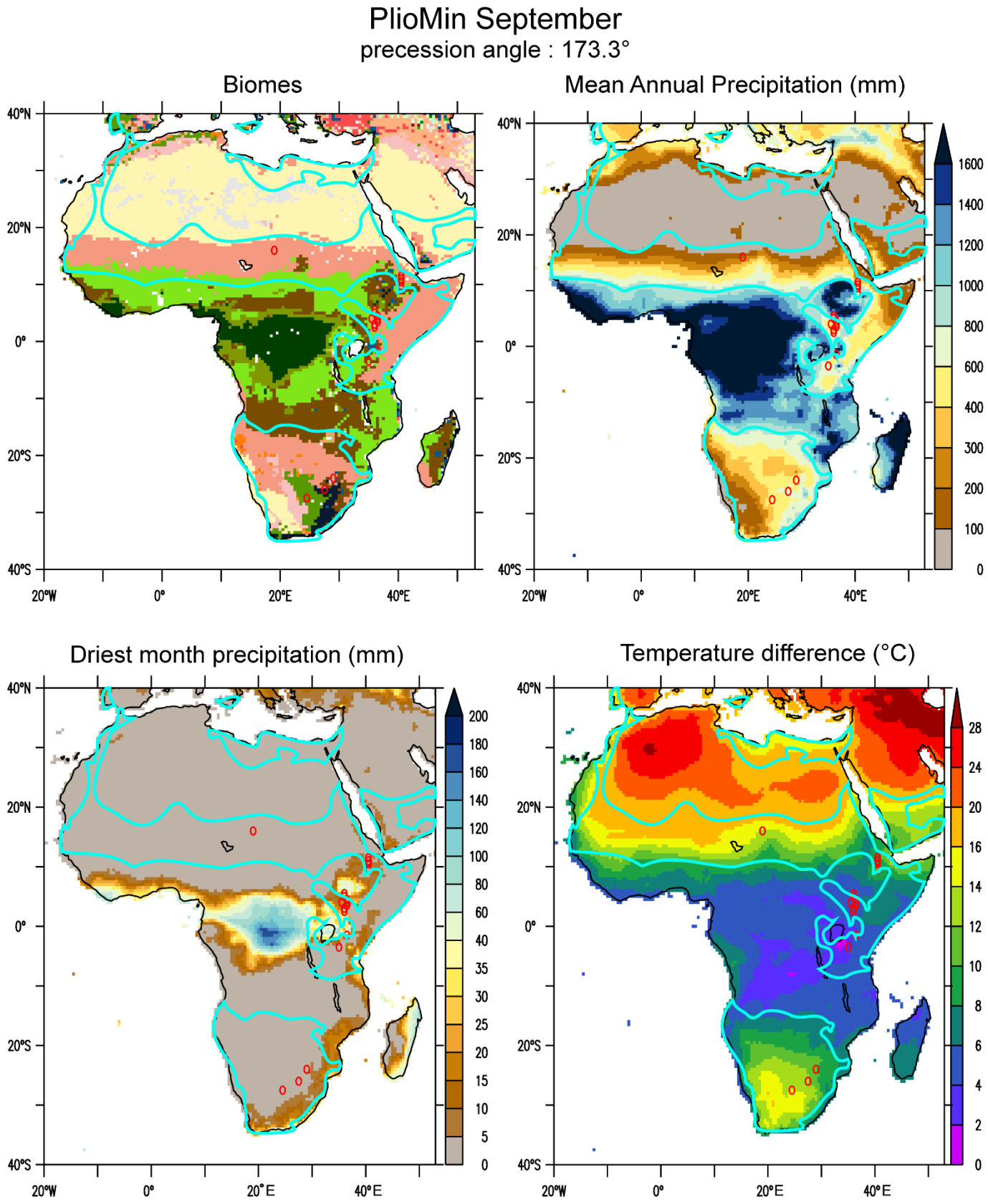

Supplementary Figure 6. Biomes, Mean annual precipitation (MAP), driest month precipitation (DMP), temperature difference between the coldest and warmest months (DT). Areas suitable for hominins from figure 4 PlioMin September final model are marked by contours.

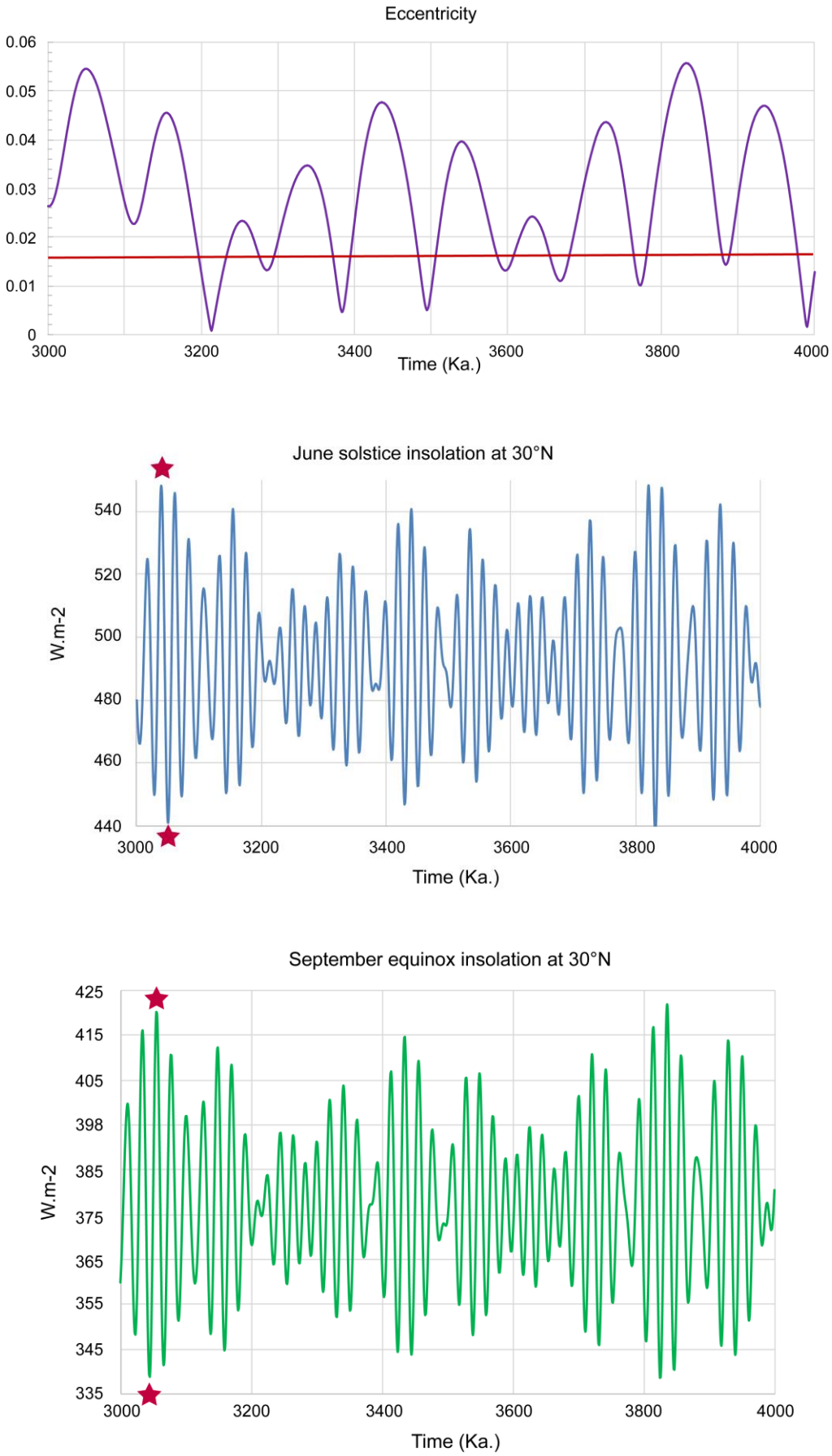

Supplementary Figure 7. Orbital eccentricity, June solstice and September equinox insolation at 30°N from 3 to 4 Ma (Laskar 2004). Red lines represent the values used for the Pliocene 'mean' climate (present-day values). Red stars indicate values chosen for orbital climate simulations.

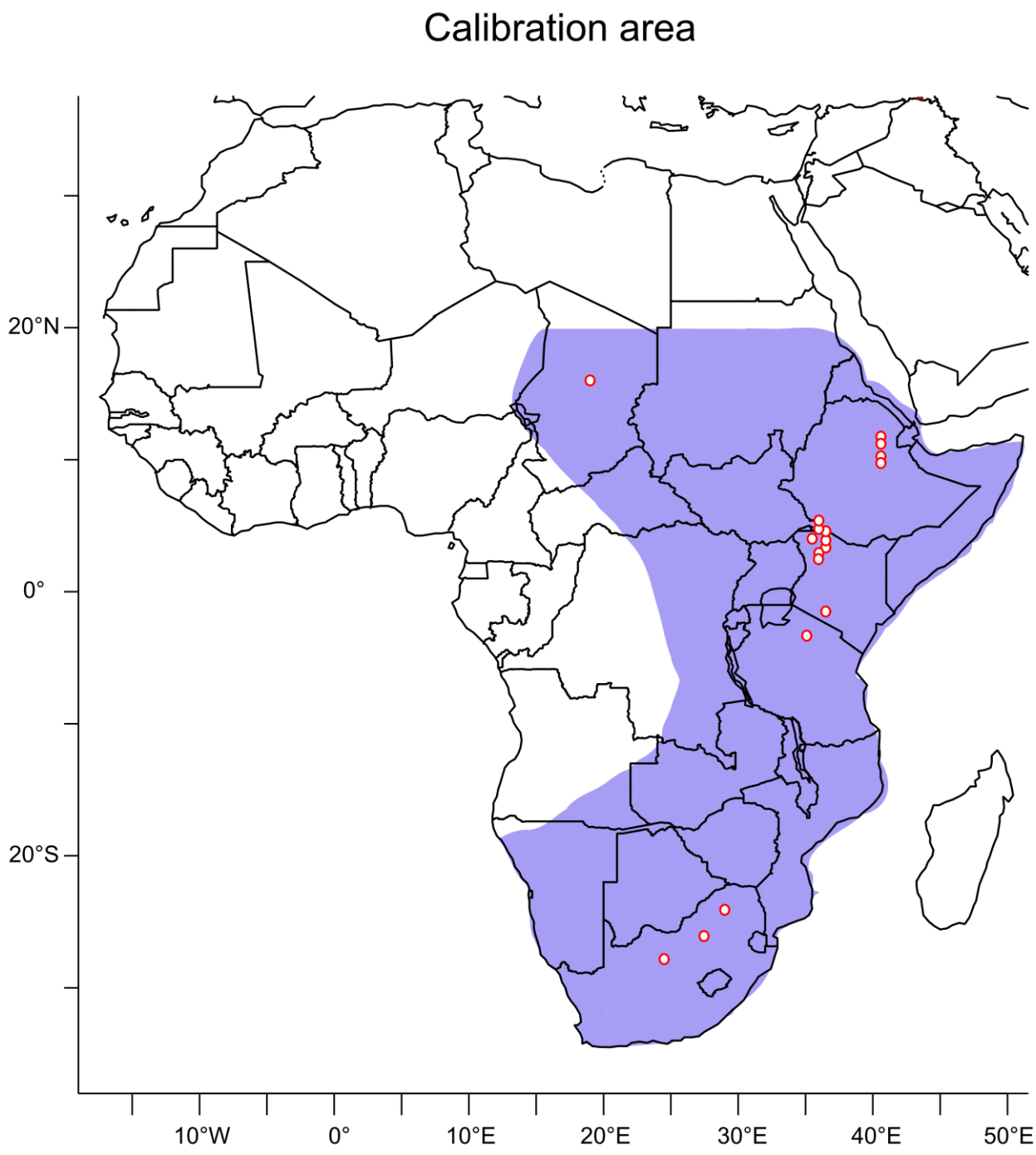

Supplementary Figure 8. Calibration area. The purple area is used to compute KUENM-Maxent model, the probability distribution associated with occurrences is compared with background points randomly sampled in the environment within calibration area. It should encompass all occurrences points, but should not be too large to avoid model overfitting.

Supplementary Table 1. Model-data comparison at hominin sites.

Site	Modeled biome	Data-inferred paleovegetation	Water resource
Koro-Toro	Tropical xerophytic shrubland	Gallery forest, wooded savannah, open grassland (Fara et al. 2005, Novello et al. 2017)	Freshwater lake (Schuster et al. 2009, Novello et al. 2017)
Woranso-Mille	Tropical xerophytic shrubland	Swamp, open woodland, grassland (Behrensmeyer & Reed 2013), riparian forest (Saylor et al., 2019)	River, springs (Haile-Selassie et al. 2007, Barboni et al. 2019), lake (Saylor et al., 2019)
Hadar & Dikika	Tropical xerophytic shrubland	Tropical xerophytic shrubland (Bonnefille et al., 2004), open grassland (Behrensmeyer & Reed 2013)	River, lake (Taieb et al., 1975)
Middle Awash	Tropical xerophytic shrubland	Grassy woodland-bushland (Behrensmeyer & Reed 2013)	
Galili	Tropical xerophytic shrubland	Woodland to bushland with some open grassland (Behrensmeyer & Reed 2013, Kullmer 2008)	
Usno	Tropical savanna	Ecotonal environment at the edge of woodland and grassland (Bobe 2011)	River (Bobe 2011)
Shungura	Tropical xerophytic shrubland	Same as Usno	Same as Usno
Fejej	Tropical xerophytic shrubland	unknown	
Koobi Fora	Tropical xerophytic shrubland	Tropical savannah (Salzmann et al. 2008)	Floodplain (Behrensmeyer & Reed 2013)
Allia Bay	Tropical xerophytic shrubland	Seasonal, mosaic of woodland-grassland (Behrensmeyer & Reed 2013)	
Lomekwi	Tropical xerophytic shrubland	Tropical deciduous woodland (Salzmann et al. 2008)	Fluvio-lacustrine (Boyd et al. 2018)
Lothagam	Tropical xerophytic shrubland	Dry and seasonally open (Behrensmeyer & Reed 2013)	
Kanapoi	Tropical xerophytic shrubland	Grassy woodland (Quinn & Lepre 2018), shrub savannah (Head & Muller 2018)	Lake, river margin (Head & Muller 2018)
Kantis	Tropical deciduous woodland	Mosaic of woodland, shrubland, grassland (Mbua et al. 2016)	
Laetoli	Tropical savanna	mosaic of woodland, bushland, shrubland, grassland (Su & Croft 2018)	River margin (Su & Croft 2018), probable springs (Barboni et al. 2019)
Makapansgat	Tropical xerophytic shrubland	Mosaic of riparian woodland, bushland, edaphic grassland (Reed 1997)	River or spring (Behrensmeyer & Reed 2013)
Sterkfontein	Warm mixed forest	Temperate sclerophyll woodland (Salzmann et al. 2008), riparian forest, bushland (Behrensmeyer & Reed 2013)	
Taung	Temperate sclerophyll woodland	Dense woodland (Behrensmeyer & Reed 2013)	Spring (McKee & Kuykendall, 2016, review in Barboni et al., 2019)

Koro-Toro site, Chad

Fara et al., (2005) conclude that *"paleoenvironments were heterogeneous"*, with *"lakeside environments surrounded by a patchwork of gallery forest, wooded savannah and open grassland"*. Diatom data indicate freshwater lake, and phytolith data confirm the heterogeneous pattern and abundance of C_4 grasses (Novello et al. 2017). The model simulates tropical xerophytic shrubland, here dominated by tropical raingreen trees and C_4 grasses, with some woody desert plants, corresponding to the vegetation reconstructions. There is also evidence of lacustrine conditions (Schuster et al., 2009) at Koro-Toro site. A lake large enough would have locally impacted surrounding vegetation, even to a larger extent than gallery forest, especially on its eastern side, where the hominin site is located and where precipitation could have been increased by the presence of the lake (Contoux et al., 2013).

Awash Basin, Ethiopia

For the Awash sites, the model simulates tropical xerophytic shrubland for which the LAI of tropical raingreen trees is between 2.51 and 3.13, i.e. values typical of open woodlands. Data describe mosaic environments mixed C_3-C_4, grassy woodlands and bushlands (Behrensmeyer and Reed, 2013) likely to correspond to tropical savanna or to tropical xerophytic shrubland. In the model, tropical savannah (for which LAI must be superior to 4 in the model) is simulated on the grid cells located just to the west of each Afar site (Fig. 1), in agreement with plausible greater humidity and cooler temperature on the escarpments, which even today sustains a slightly more wooded and green vegetation compared to the lowlands.

Turkana Basin

At Usno the model simulates tropical savannah. For all the other sites in the Turkana basin, the model simulates tropical xerophytic shrubland. The data suggest, similarly to the Awash basin, a mosaic of woodland and grassland, more wooded at Usno and Shungura than in the rest of the basin, in agreement with the presence of the large and permanent Omo River fluvial complex (fluvio-deltaic context at Shungura, floodplain at Koobi-Fora, fluvio-lacustrine environments at Lomekwi, Behrensmeyer and Reed 2013).

Kantis, Kenya

Mbua et al., (2016) indicate a mosaic of woodland, shrubland, grassland with more C_4 than other *Au. afarensis* sites. Here the model simulates more mesic environments than those of the Awash and of the Turkana basins, with the same mix of PFTs (tropical raingreen trees, C_4 grass and woody desert plants). All PFTs are more productive, leading to the tropical deciduous woodland biome.

Laetoli, Tanzania

Via a combination of faunal and floral analyses, Su and Croft (2018) find that vegetation at Laetoli was a *"mosaic of woodland, bushland, shrubland, grassland with riverine woodland in a relatively arid and seasonal environment"*. The review of Barboni (2014) also indicates a mosaic of dry and moist woodlands and grassland, and few components of Afromontane forest. In our study, the simulated biome at Laetoli for the Pliocene mean climate is tropical savannah, with dominant tropical raingreen trees, the presence of conifer forest, C_4 grass and woody desert plants. Thus, our simulated biome at Laetoli is consistent with the reconstructions.

South Africa

Makapansgat

The biome simulated at Makapansgat is tropical xerophytic shrubland, dominated by tropical raingreen trees, with the presence of temperate broad-leaved evergreen trees, conifer forest, C_4 grass and woody desert plants, suggesting a strong heterogeneity of the landscape. This could correspond to the habitat mosaic recognized by Reed (1997).

Sterkfontein

Salzmann et al. (2008) interpret data from Reed (1997) and Bamford (1999) as being representative of temperate sclerophyl woodland, while Reed (1997) suggests that Sterkfontein is more open than Makapansgat. Our model however simulates warm mixed forest, i.e. a landscape dominated by temperate broadleaved evergreen trees, with tropical raingreen trees, conifer forest, C_4 grass and woody desert plants. This can hardly be reconciled with the reconstructions.

Taung

Fauna suggest relatively dense woodland (Behrensmeyer and Reed, 2013) while the model simulates temperate sclerophyll woodland, i.e. a rather open landscape composed of mainly temperature broadleaved evergreen trees, conifer forest, grass and woody desert plants.

In summary, hominin sites are mostly mosaic environments of tropical trees, grasses and shrubs. Because data reconstructions are mostly qualitative, it is difficult to compare to model results, which also represents a larger spatial

scale which smoothes heterogeneity, notably because it does not include water sources. Nonetheless, the model simulates a mix of trees, grasses and shrubs at all the hominin sites, in broad agreement with reconstructions. Thus the simulated large-scale vegetation is coherent with local-scale vegetation reconstructions at hominin localities, except for Sterkfontein and Taung localities (2 sites over 18). We are therefore confident that our model's climatic variables can be used to reconstruct the *Australopithecus* climatic envelope at a broad geographic scale.

Appendix 2

R scripts for KUENM and Maxent analysis

Example script for Pliocene 'mean' climate

Computed with Rmarkdown

Environmental layers

Import of the simulated climatic layers from files beforehand cropped with calibration area (see Annexe 1) and preparation of the 2210 KUENM variables sets. "Plio_vars_noncor/var/m3_clipped" is the folder where non-correlated cropped layers are stored, "Plio_vars_noncor/FullVar" is the folder where non-cropped (all Africa) layers are stored.

```
library(kuenm)
library(raster)
library(rgeos)

setwd("yourKUENMfolder")

## preparing M variables (cropped layers for model computation)
kuenm_varcomb(var.dir = "Plio_vars_noncor/var/m3_clipped", out.dir = "M_variables", mi
n.number = 2, in.format = "ascii", out.format = "ascii")

## preparing G variables (non-cropped layers for projection of the model)
kuenm_varcomb(var.dir = "Plio_vars_noncor/FullVar", out.dir = "G_variables", min.numbe
r = 2, in.format = "ascii", out.format = "ascii")
```

Occurrences of Pliocene hominids

Import of the occurrences of Pliocene hominids living in Africa between 4 and 3 Ma, see Table 1 for references and coordinates. The 18 occurrences are then splitted in training and testing datasets to conduct model calibration. For jackknife, leave-one out approach, 18 datasets are constructed by removing one occurrence point. The models used to evaluate the impact of orbital configuration are based on the full (18) dataset.

```
## Import from .csv files
hom <- read.csv("allOccurrence.csv", sep = ";")

## Splitting in training and testing datasets
kuenm_occsplit(occ = hom, train.proportion = 0.75, method = "random", save = TRUE, nam
e = "occ")
```

Candidate models, evaluation and selection

In this step, 2210 candidate models are produced and their performance are evaluated to select the best Maxent parameterization.

```
## Parameters for model calibration

# names for directory and files
occ_joint <- "occ_joint.csv"
occ_tra <- "occ_train.csv"
M_var_dir <- "M_variables"
batch_cal <- "Candidate_models"
out_dir <- "Candidate_Models"
# regression parameters
reg_mult <- c(seq(0.1, 1, 0.1), seq(2, 6, 1), 8, 10)
f_clas <- c("q", "lq", "lp", "qp", "lqp")
args <- NULL
```

```
maxent_path <- "C:/Maxent"
wait <- FALSE

run <- TRUE
occ_test <- "occ_test.csv"
out_eval <- "Calibration_results"
threshold <- 5
rand_percent <- 50
iterations <- 100
kept <- TRUE
selection <- "OR_AICc"
paral_proc <- FALSE

## Computation of the candidate models
kuenm_cal(occ.joint = occ_joint, occ.tra = occ_tra, M.var.dir = M_var_dir, batch = bat
ch_cal, out.dir = out_dir, reg.mult = reg_mult, f.clas = f_clas, args = args, maxent.p
ath = maxent_path, wait = wait, run = run)

## Computation of model evaluation and selection
cal_eval <- kuenm_ceval(path = out_dir, occ.joint = occ_joint, occ.tra = occ_tra, occ.
test = occ_test, batch = batch_cal, out.eval = out_eval, threshold = threshold, rand.p
ercent = rand_percent, iterations = iterations, kept = kept, selection = selection, pa
rallel.proc = paral_proc)
```

Final models

Computation of the final models and projection on G_variables (i.e. the entire Africa)

```
batch_fin <- "Final_models"
mod_dir <- "Final_Models"
rep_n <- 10
rep_type <- "Bootstrap"
jackknife <- FALSE
out_format <- "logistic"
project <- TRUE
G_var_dir <- "G_variables"
ext_type <- "all"
write_mess <- FALSE
write_clamp <- FALSE
wait1 <- FALSE
run1 <- TRUE
args <- NULL

kuenm_mod(occ.joint = occ_joint, M.var.dir = M_var_dir, out.eval = out_eval, batch = b
atch_fin, rep.type = rep_type, jackknife = jackknife, out.dir = mod_dir, out.format =
out_format, project = project, G.var.dir = G_var_dir, ext.type = ext_type, write.mess
= write_mess, write.clamp = write_clamp, maxent.path = maxent_path, args = args, wait
= wait1, run = run1)
```

Computation of extrapolation risk analysis

As with any model fitting exercise, interpretation of model predictions outside the range of the independent variables on which models were calibrated is perilous. To estimate the extrapolation risk we use Mobility-Oriented Parity (MOP) analysis (Owen et al. 2013)

```
sets_var <- c("Set_8") #these are the variable combo sets used in Final models
out_mop <- "MOP_results"
percent <- 10
swd <- FALSE
paral <- FALSE
```

```
kuenm_mmop(G.var.dir = G_var_dir, M.var.dir = M_var_dir, is.swd = swd, sets.var = sets
_var, out.mop = out_mop, percent = percent, parallel = paral)

# MOP summary
dir.create("MOP_summary")

mops <- stack(list.files(out_mop, pattern = ".tif$", full.names = TRUE, recursive = TR
UE))

meam <- calc(mops, mean)
minm <- calc(mops, min)

writeRaster(meam, filename = "MOP_summary/Mean_MOP.tif", format = "GTiff")
writeRaster(minm, filename = "MOP_summary/Min_MOP.tif", format = "GTiff")
```

Computation of final model statistics

Last step of the KUENM analysis, caution incorrect sp_name and scenarios variables can prevent the analysis from running. The final model can be projected on multiples environmental layers by adding their names in “scenarios” variable (e.g. “Africa”, “PlioMin June”, “PlioMin September”) and the respective layers in G_variables.

```
# Model statistics: The final models to be analyzed will be found in the Final_Model_S
tats folder.
format <- "asc"
project <- TRUE
stats <- c("med", "range", "avg")
rep <- TRUE
# the type of extrapolation can be selected according to user requirements
ext_type <- c("E", "EC", "NE")
out_dir <- "Final_Model_Stats"

# Select names of taxa name in occurrence file and G_variable name (i.e. Africa)
sp_name <- "Hominin"
scenarios <- c("Africa")

kuenm_modstats(sp.name = sp_name, fmod.dir = mod_dir, format = format, project = proje
ct,
               statistics = stats, replicated = rep, proj.scenarios = scenarios,
               ext.type = ext_type, out.dir = out_dir)
```

Figure 1

Click here to access/download;Figure;Fig.1 Biomes simulated with Pliocene mean climate.pdf

Biomes simulated with Pliocene mean climate

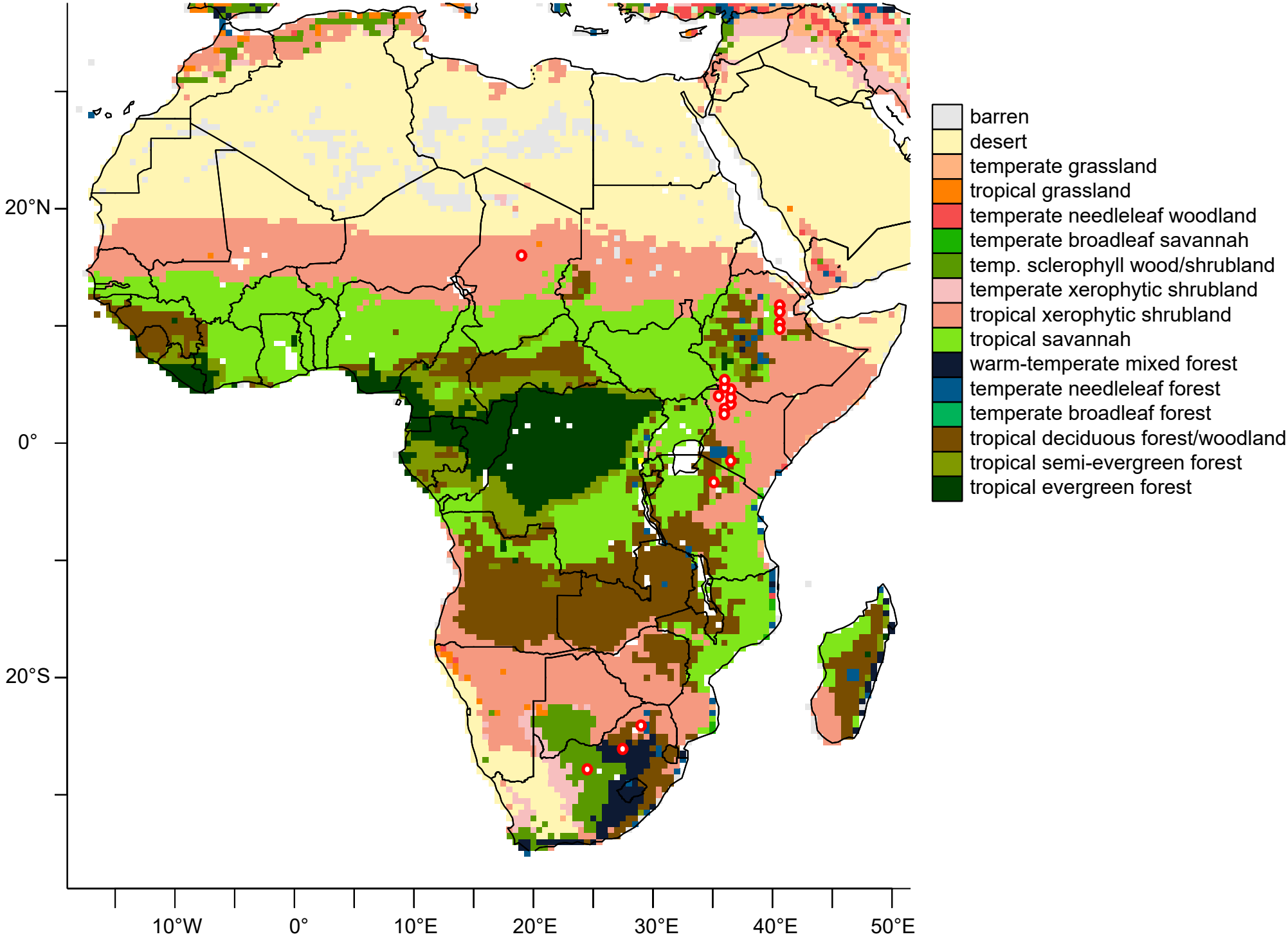

Figure 2

Final habitat suitability model for hominins

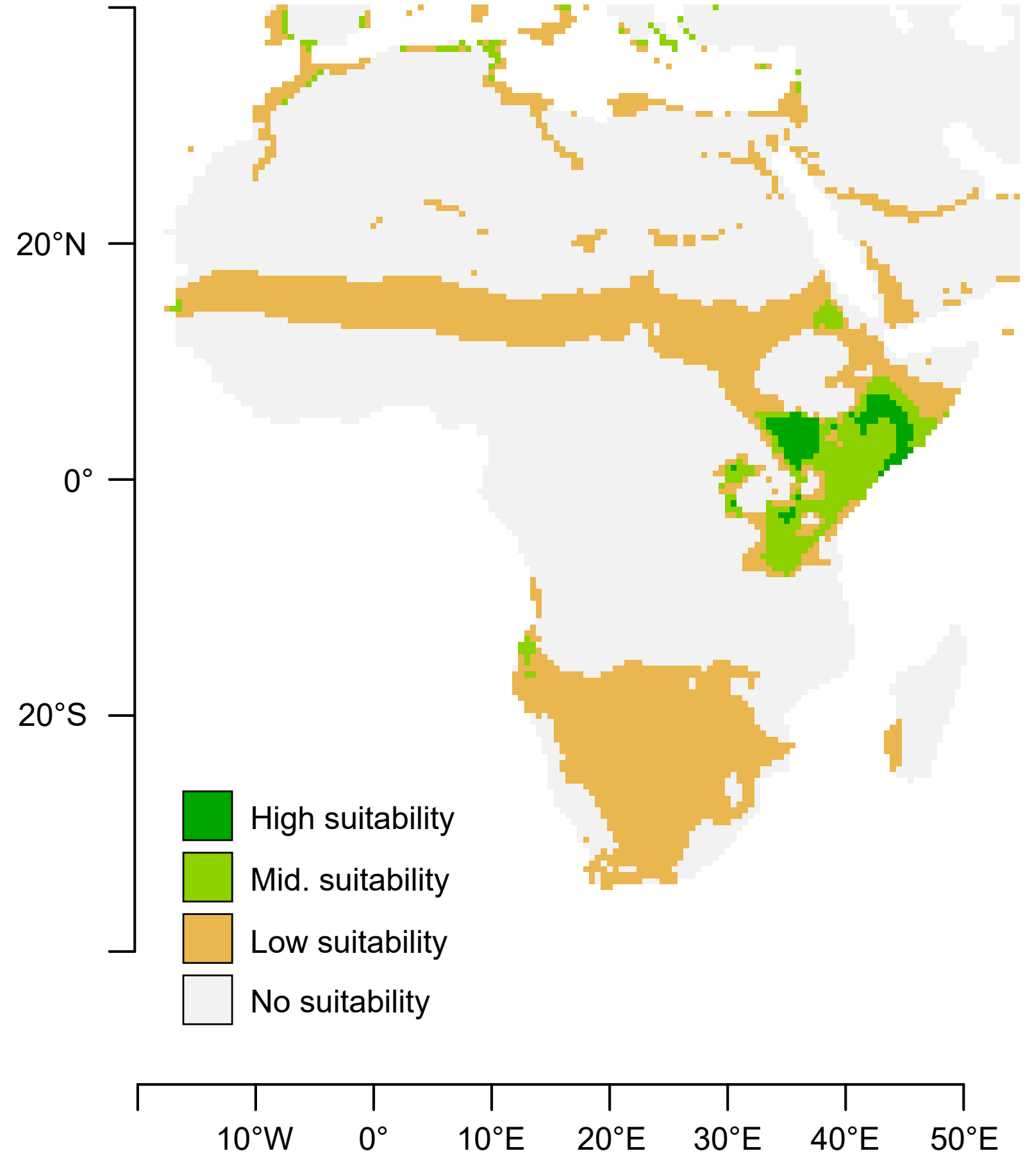

Figure 3

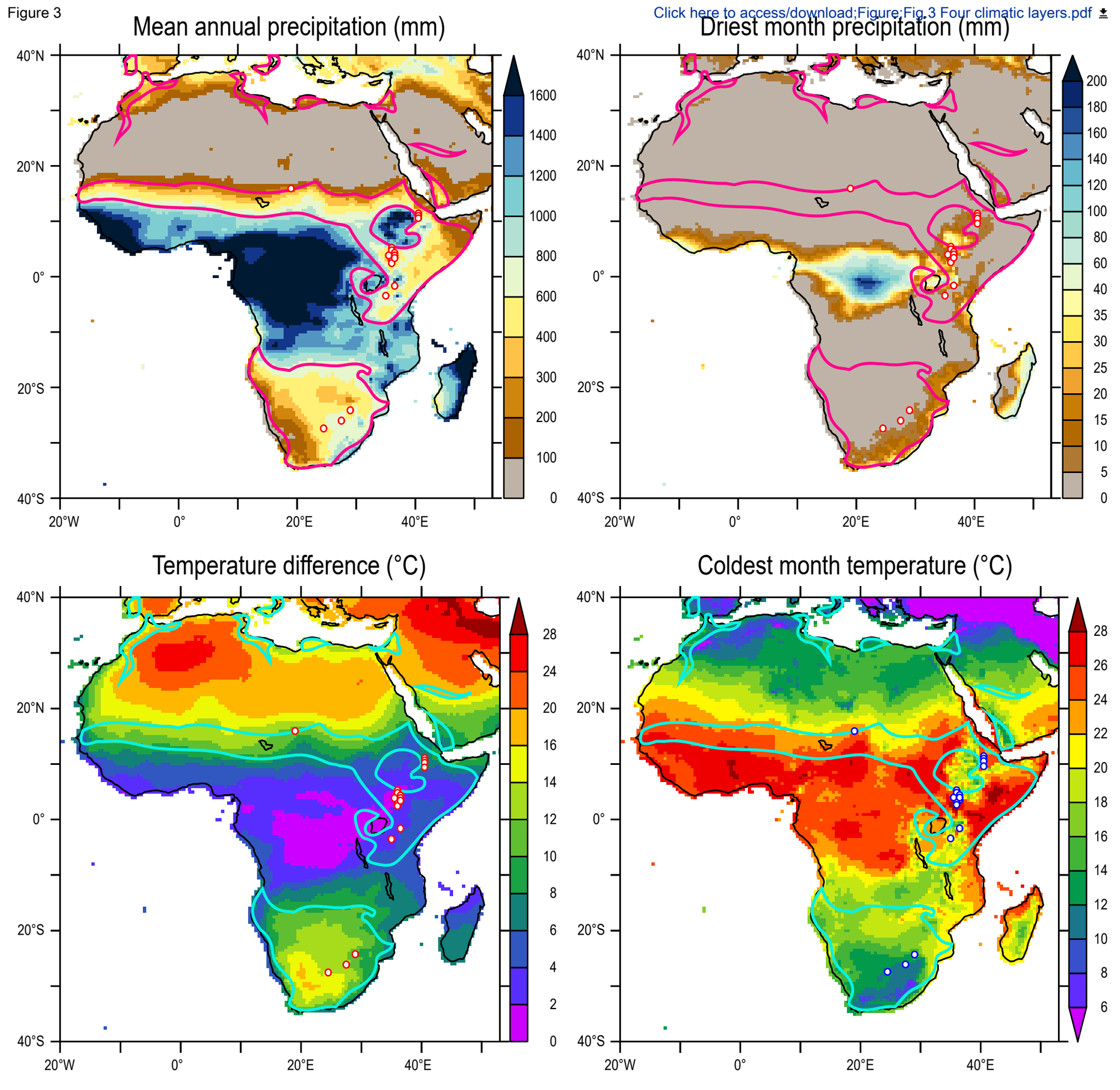

Figure 4

Click here to access/download;Figure;Fig

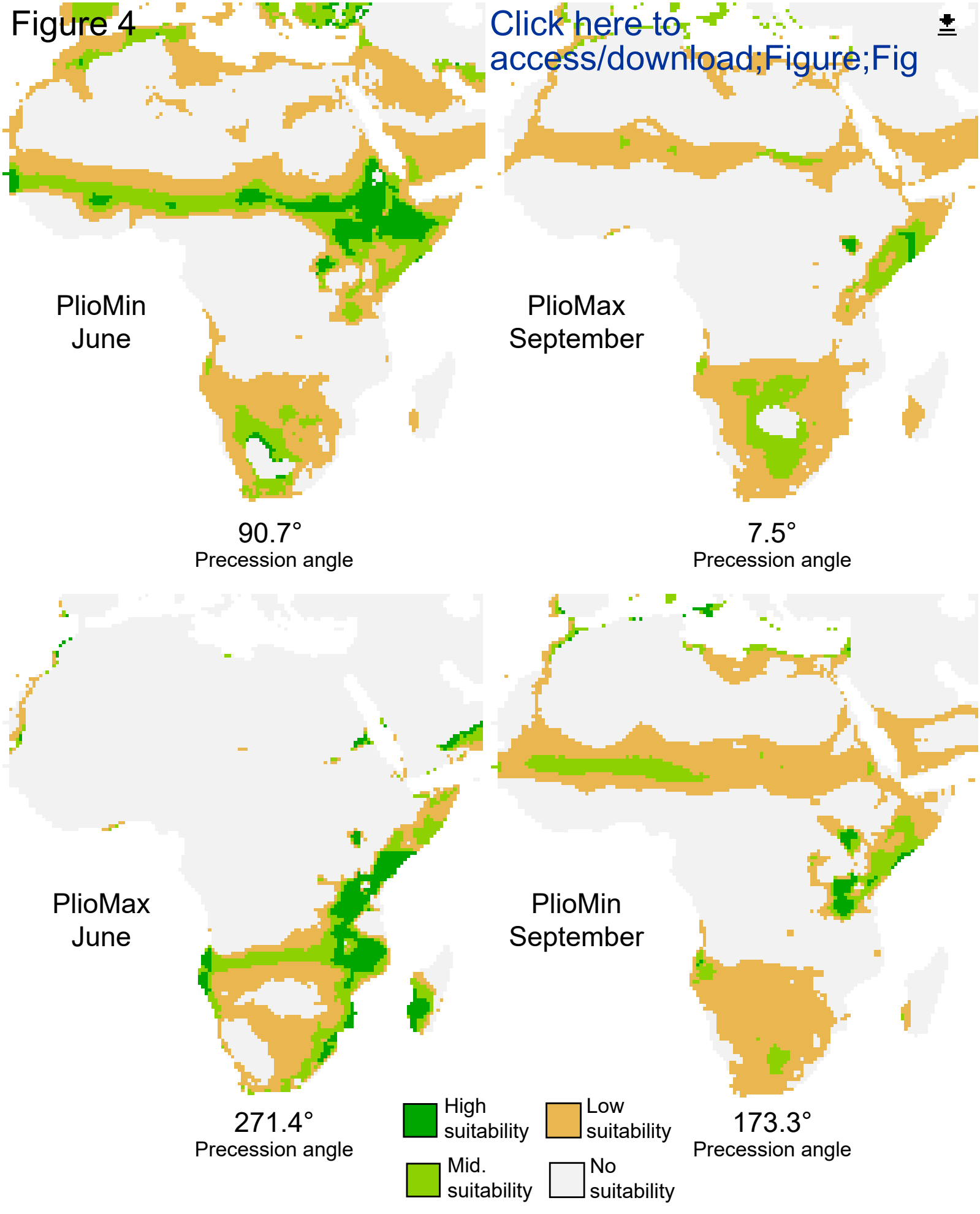

Figure 5

Consensus map of the four orbital precession projections and Pliocene 'mean' climate model